Timing and Synchronization - II

A. Gallo

Istituto Nazionale di Fisica Nucleare Laboratori Nazionali di Frascati

via Enrico Fermi 40 - 00044 Frascati(RM) - Italy

Lecture I&II Outline

Lecture I

- **MOTIVATIONS**
  - ✓ Why accelerators need synchronization, and at what precision level
- **DEFINITIONS AND BASICS**
  - ✓ Glossary: Synchronization, Master Oscillator, Drift vs. Jitter
  - ✓ Fourier and Laplace Transforms, Random processes, Phase noise in Oscillators
  - ✓ Phase detectors, Phase Locked Loops, Precision phase noise measurements

Lecture II

  - ✓ Electro-optical and fully optical phase detection
- **SYNCRONIZATION ARCHITECTURE AND PERFORMANCES**
  - ✓ Phase lock of synchronization clients (RF systems, Lasers, Diagnostics, ...)
  - ✓ Residual absolute and relative phase jitter
  - ✓ Reference distribution – actively stabilized links
- **BEAM ARRIVAL TIME FLUCTUATIONS**
  - ✓ Bunch arrival time measurement techniques
  - ✓ Expected bunch arrival time downstream magnetic compressors (an example)
  - ✓ Beam synchronization – general case

CONCLUSIONS AND REFERENCES

BASICS

- *Electro-optical phase detection*
- *Fully-optical phase detection*

Phase detection between RF and Laser: photodiode optic-to-RF conversion

Straightforward approach to measure the phase of a laser pulse train against an RF oscillator voltage is to ***convert the light pulses into electric signals*** by means of a ***fast photodiode***. The electric pulses have the same laser rep rate and the spectrum of the signal is a comb made by all the harmonics of the laser fundamental frequency up to the photodiode band limit (that can extend to many GHz, while the spectrum of the original laser can extend well beyond 1 THz). ***One specific harmonic*** of the laser converted spectrum can be ***extracted*** with a ***bandpass filter***, to obtain a sine wave to be ***phase compared*** with an RF oscillator by means of standard devices (such as an RF mixers).

It is a ***simple*** and ***effective*** method. However, it suffers from ***temperature sensitivity*** and ***AM to PM conversion*** in the photodiode.

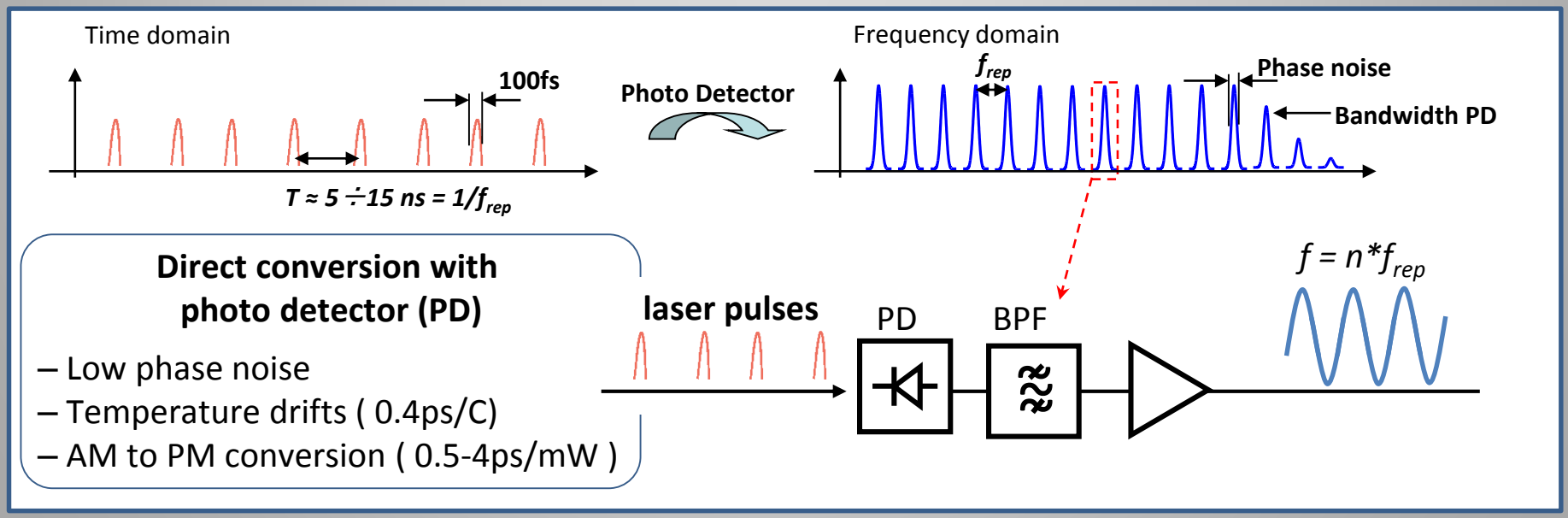

Phase detection between RF and Laser: Sagnac Loop Interferometer or BOM-PD

(Balanced Optical Microwave Phase Detector)

Recently (≈ 10 years) a special device to perform direct measurements of the ***relative phase*** between an ***RF sine-wave*** and a ***train of short laser pulses*** has been developed based on a ***Sagnac-loop interferometer*** ring including a directional electro-optic phase modulator. The BOM-PD is capable to ***convert*** the ***phase error*** between a laser pulse train and a μwave oscillator in an ***amplitude modulation*** of the laser pulse train downstream the interferometer, that can be voltage converted by a photodiode.

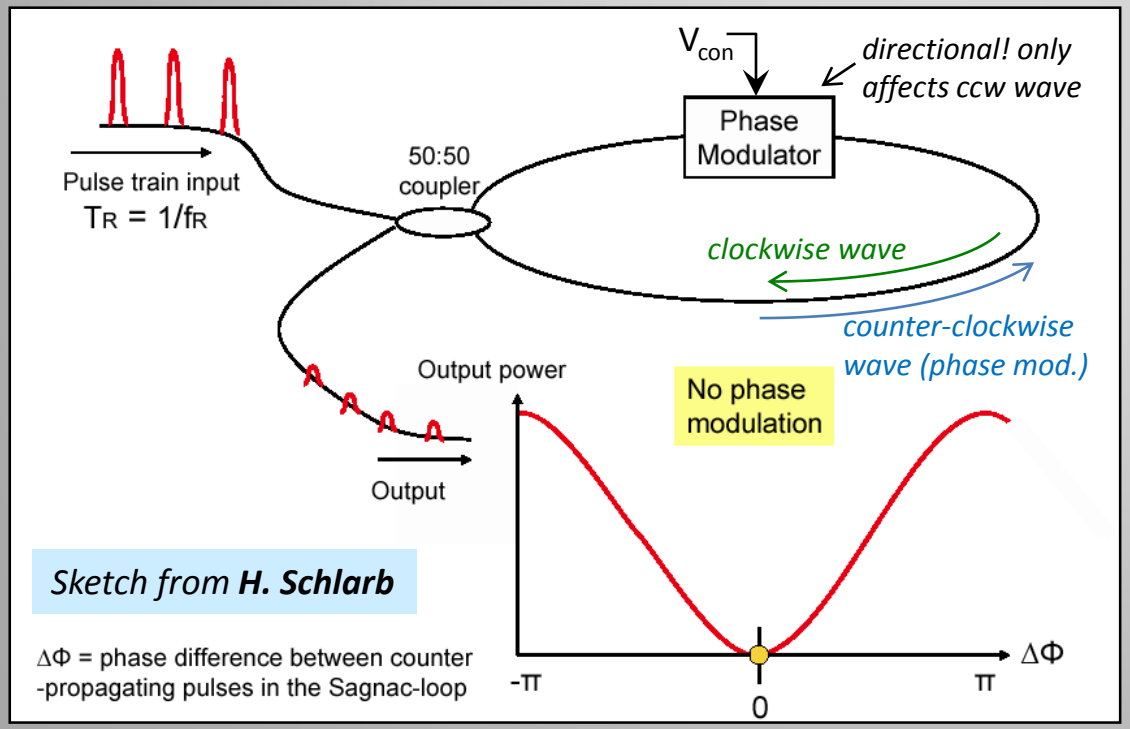

The electro-optic modulator produces a dephasing $\Delta\Phi$ between the optical carriers of the 2 counter-propagating pulse trains proportional to the applied control voltage V_{con}. The intensity I_{out} of the laser train emerging from the interferometer is then:

$$I_{out} \div I_{in}\overline{[\cos(\omega_c t) - \cos(\omega_c t + \Delta\Phi)]^2} \div \div I_{in}\sin^2(\Delta\Phi/2)$$

If no voltage is applied at the modulator control port then $\Delta\Phi = 0$ and the 2 counter-propagating waves interfere destructively at the output combiner.

The amplitude of the output pulses is nearly zero in this case.

Sagnac Loop Interferometer or BOM-PD

The phase modulator needs to be ***biased*** by a sine wave voltage of ***frequency*** $f_R/2$, being f_R the laser repetition frequency. The $f_R/2$ sine wave is obtained from the input pulse train, and has to be phased such that the laser pulses cross the modulator aligned with the sine wave maxima and minima.

Under this condition the ***pulses experience in sequence a phase shift of*** $\pm\Delta\Phi_0$. The intensity of the laser output train is non-zero in this case, but it does not show amplitude modulation since all pulses are equally attenuated.

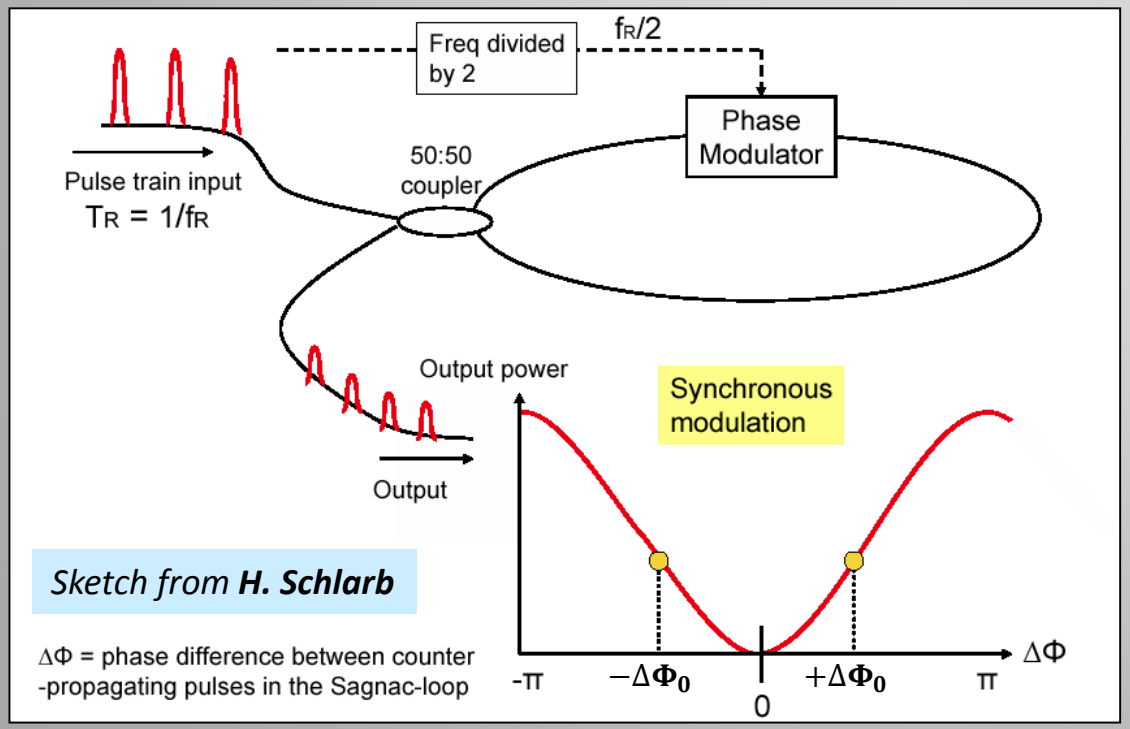

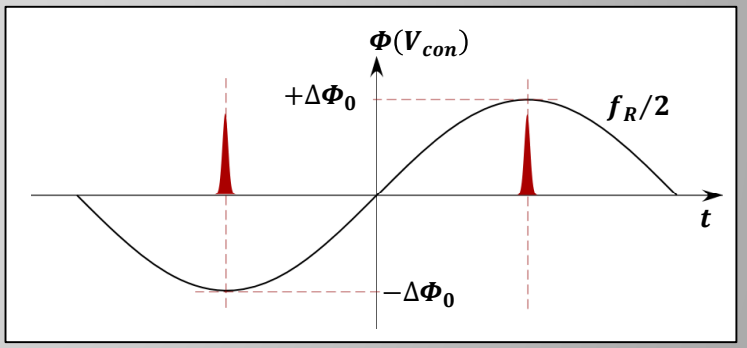

Sagnac Loop Interferometer or BOM-PD

Let's add on the modulator control port a ***sine wave voltage of frequency*** Nf_R, an integer multiple of the laser repetition frequency. The harmonic voltage will imprint a constant contribution θ_e to the phase of all pulses, so finally the pulses will show in sequence a phase modulation equal to $\theta_e \pm \Delta\Phi_0$. The intensities of "even" and "odds" pulses emerging from the interferometer are different, so the ***output pulse train is amplitude modulated***, with a modulating frequency $f_R/2$ and a ***modulation depth*** depending on the ***relative phase*** between the ***harmonic voltage*** and the ***input laser train***.

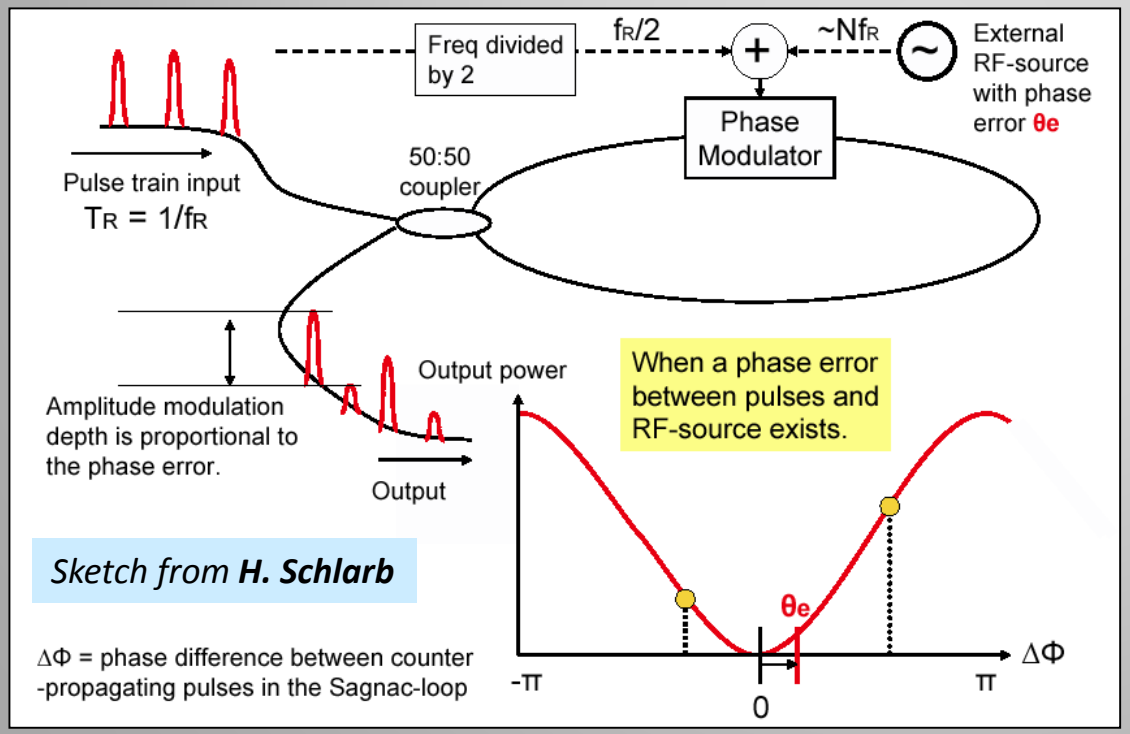

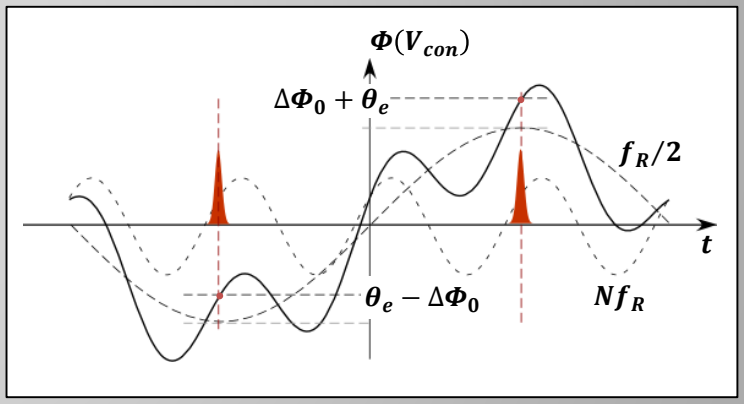

Sagnac Loop Interferometer or BOM-PD

The ***output laser*** pulse train is ***amplitude demodulated*** to extract the ***phase error information***. A possible use of the phase error signal is driving a PLL to lock a VCO tuned around one harmonic of the original laser repetition rate f_R. This configuration allows ***extracting*** and converting to a μwave signal the ***timing information encoded in the laser rep rate***, with the best preservation of the phase purity.

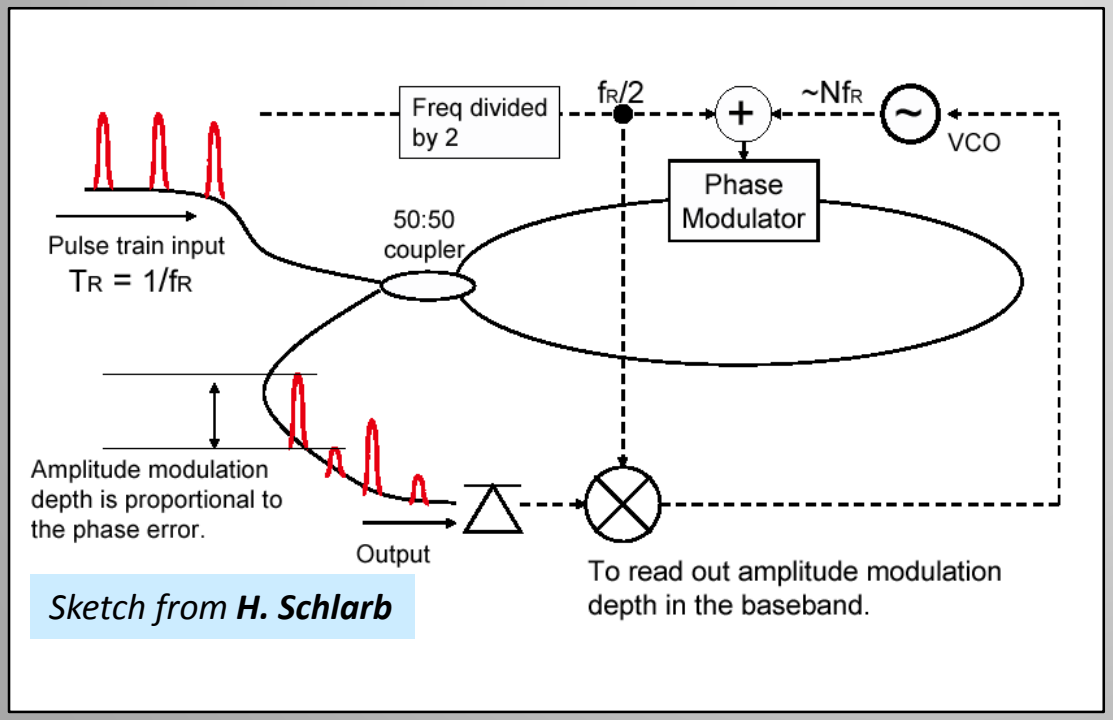

*Sketch from **H. Schlarb***

Balanced optical mixer to lock RF oscillators

– insensitive against laser fluctuation
– very low temperature drifts

Results: f=1.3GHz jitter & drift <10 fs rms ***limited by detection!***

Optical vs. Optical

Balanced cross correlation of very short optical pulses ($\sigma_t \approx 200\ fs$) provides an ***extremely sensitive*** measurement of the ***relative delay between*** 2 pulses.

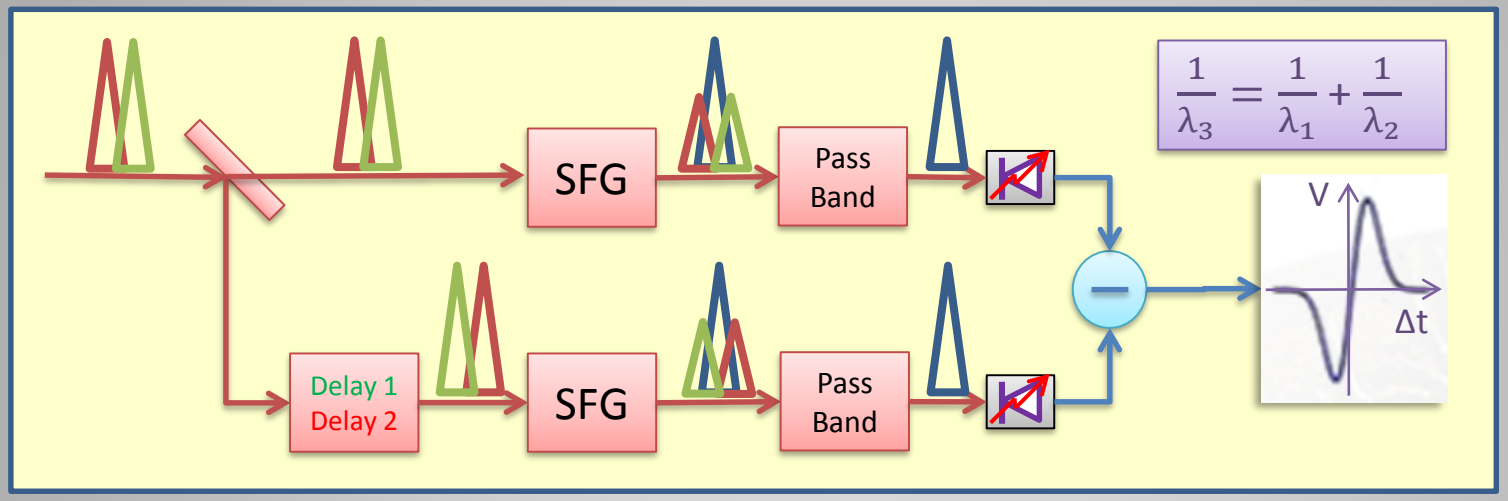

The two pulses have orthogonal polarization and generate a shorter wavelength pulse proportional to their time overlap in each branch by means of non-linear crystal.

In a second branch the two polarizations experience a differential delay $\Delta T = T_1 - T_2 \approx \sigma_t$. The amplitudes of the interaction radiation pulses are converted to voltages by photodiodes and their difference is taken as the detector output V_0.

If the initial time delay between the pulses is exactly $\Delta T/2$ then clearly $V_0 \approx 0$ (balance), while it grows rapidly as soon as initial delay deviates.

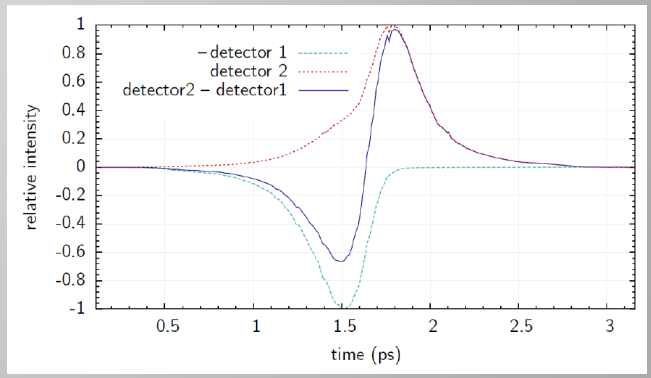

Detection sensitivity up to 10 mV/fs achievable with ultra-short pulses!!!

Performances of Synchronization Systems

- *Client Residual Jitter*
- *Stabilized Reference Distribution*

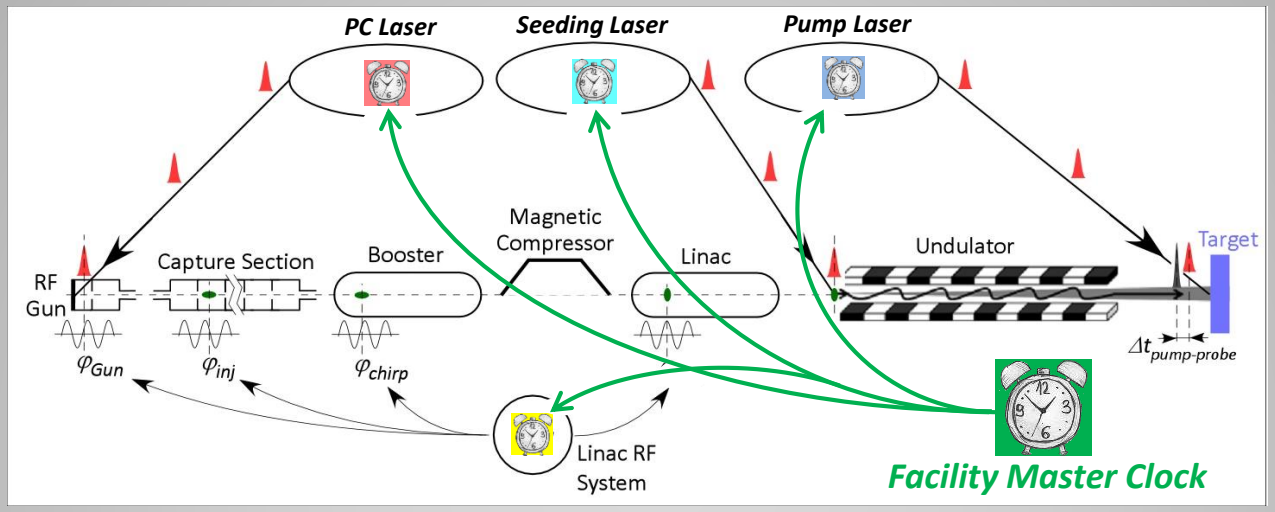

A client with a free-run phase noise φ_{i_0} once being PLL locked to the reference with a loop gain $H_i(j2\pi f)$ will show a residual phase jitter φ_i and a phase noise power spectrum S_i according to:

$$\varphi_i = \frac{H_i}{1+H_i}\varphi_{ref} + \frac{1}{1+H_i}\varphi_{i_0} \rightarrow \quad S_i(f) = \frac{|H_i|^2}{|1+H_i|^2}S_{ref}(f) + \frac{1}{|1+H_i|^2}S_{i_0}(f)$$

Uncorrelated noise contributions

Client absolute residual time jitter

$$\sigma_{t_i}^2 = \frac{1}{\omega_{ref}^2}\int_{f_{min}}^{+\infty}\frac{|H_i|^2 S_{ref}(f) + S_{i_0}(f)}{|1+H_i|^2}df$$

But we are finally interested in relative jitter between clients and reference $\varphi_{i-r} = \varphi_i - \varphi_{ref}$, and among different clients $\varphi_{i-j} = \varphi_i - \varphi_j$:

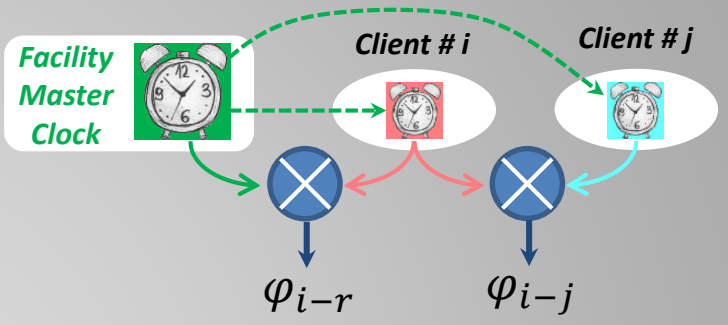

$$\varphi_{i-r} = \frac{\varphi_{i_0} - \varphi_{ref}}{1 + H_i} \rightarrow S_{i-r}(f) = \frac{S_{i_0}(f) + S_{ref}(f)}{|1 + H_i|^2}$$

Client residual relative time jitter $\quad \sigma^2_{t_{i-r}} = \frac{1}{\omega^2_{ref}} \int_{f_{min}}^{+\infty} \frac{S_{ref}(f) + S_{i_0}(f)}{|1 + H_i|^2} df$

$$\varphi_{i-j} = \frac{\varphi_{i_0} - \varphi_{ref}}{1 + H_i} - \frac{\varphi_{j_0} - \varphi_{ref}}{1 + H_j} \rightarrow S_{i-j}(f) = \frac{S_{i_0}(f)}{|1 + H_i|^2} + \frac{S_{j_0}(f)}{|1 + H_j|^2} + \left|\frac{H_i - H_j}{(1 + H_i)(1 + H_j)}\right|^2 S_{ref}(f)$$

$$\sigma^2_{t_{i-j}} = \frac{1}{\omega^2_{ref}} \int_{f_{min}}^{+\infty} S_{i-j}(f)\, df$$

Residual relative time jitter between clients i-j

If $H_i \neq H_j$ there is a **direct contribution** of the **master clock phase noise** $S_{ref}(f)$ to the **relative jitter** between clients *i* and *j* in the region between the cutoff frequencies of the 2 PLLs. That's why **a very low RMO phase noise** is specified in a **wide spectral region** including the cut-off frequencies of all the client PLLs (0.1÷100 kHz typical).

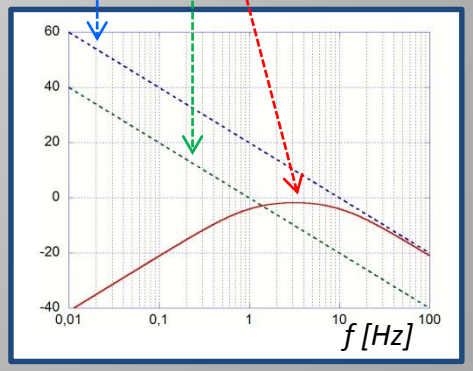

Drift of the reference distribution

Client ***jitters*** can be reduced by ***efficient PLLs*** locking to a local copy of the reference.

Reference distribution ***drifts*** need to be ***under control*** to preserve a good facility synchronization.

Depending on the facility size and specification the reference distribution can be:

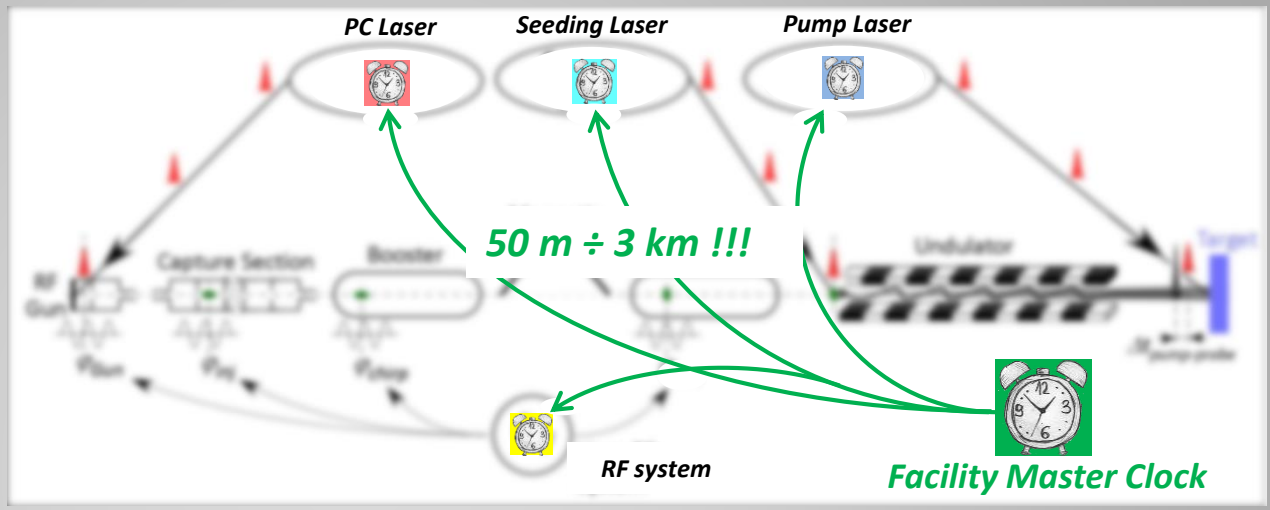

RF based, through coaxial cables

- ✓ *Passive (mainly) / actively stabilized*
- ✓ *Cheap*
- ✓ *Large attenuation at high frequencies*
- ✓ *Sensitive to thermal variations (copper linear expansion ≈ 1.7 10^{-5}/°C)*
- ✓ *Low-loss 3/8" coaxial cables very stable for ΔT<<1°C @ T_0≈ 24 °C*

Optical based, through fiber links

- ✓ *Pulsed (mainly), also CW AM modulated*
- ✓ *High sensitivity error detection (cross correlation, interferometry, ...)*
- ✓ *Small attenuation, large BW*
- ✓ *Expensive*
- ✓ *Active stabilization always needed (thermal sensitivety of fibers)*
- ✓ *Dispersion compensation always needed for pulsed distribution*

Drift of the reference distribution

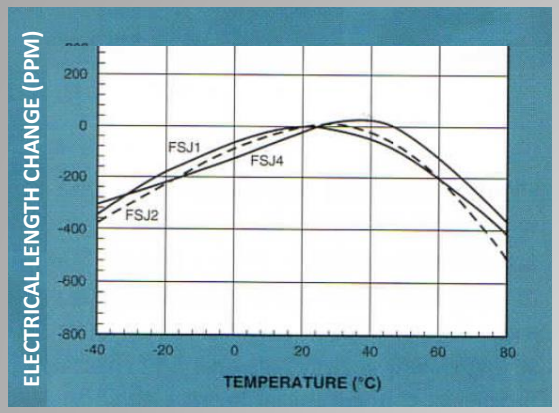

Around some optimal temperature T_{opt} cable physical elongation is compensated by dielectric constant variation. PPM relative delay variation is:

$$\left.\frac{\Delta\tau}{\tau}\right|_{PPM} \approx -\left(\frac{T - T_{opt}}{T_c}\right)^2$$

For a 3/8" cable (FSJ2): $T_{opt} \approx 24\,°C$, $T_c \approx 2\,°C$. Good enough?

$$L \approx 1\,km \rightarrow \tau \approx 5\,\mu s \rightarrow \Delta\tau/\tau \approx 5fs/5\mu s \approx 10^{-3} PPMs$$!!!

LONG DISTANCES ➡ ***ACTIVE LINK STABILIZATION REQUIRED !!!***

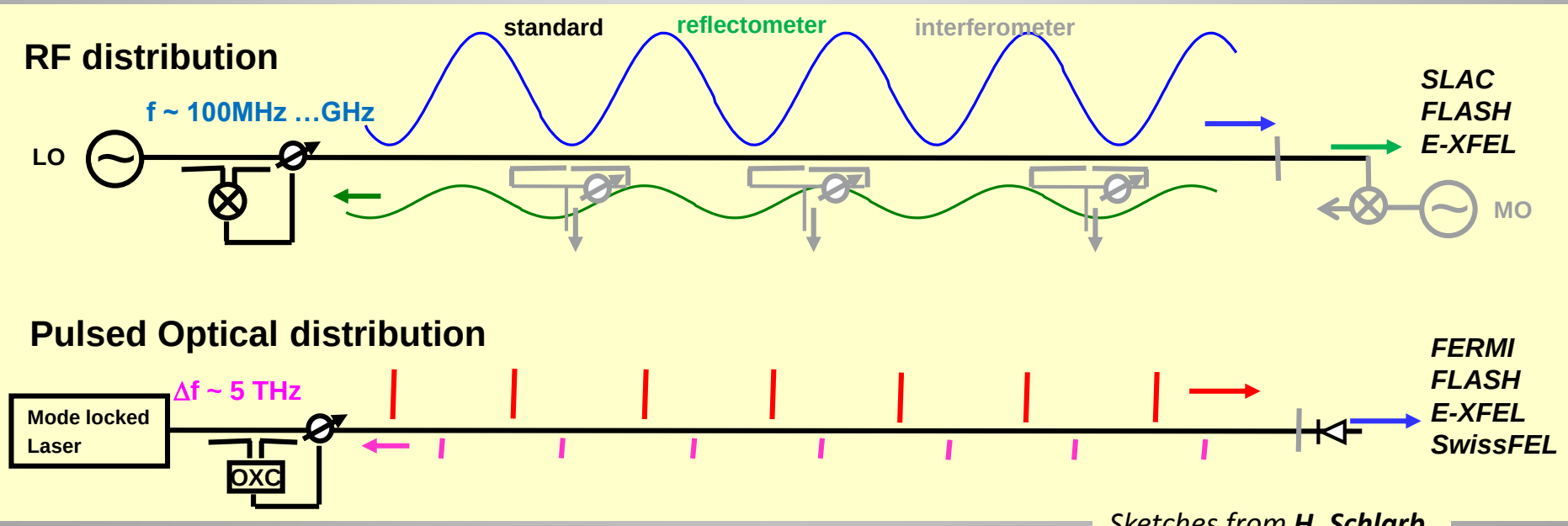

*Sketches from **H. Schlarb***

Drift of the reference distribution

Active stabilized links are based on high resolution ***round trip time measurements*** and ***path length correction*** to stick at some stable reference value.

Pulsed optical distribution is especially suitable, because of low signal attenuation over long links and path length monitoring through very sensitive pulse cross-correlators. However, ***dispersion compensation of the link is crucial*** to keep the optical pulses very short ($\approx 100\ fs$).

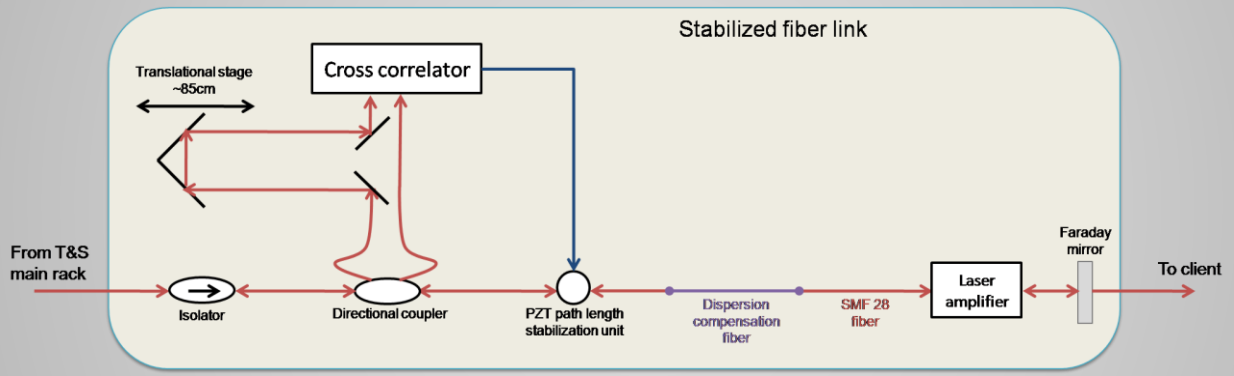

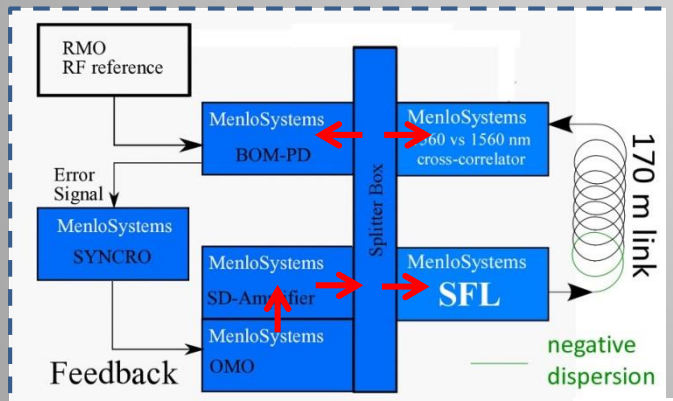

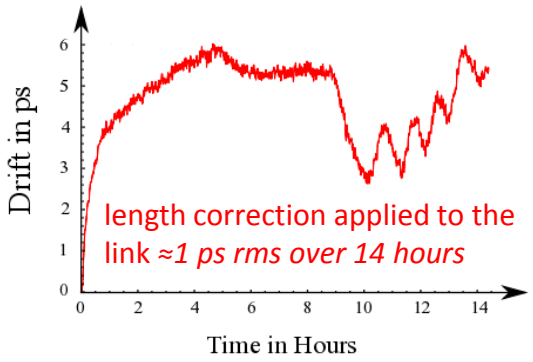

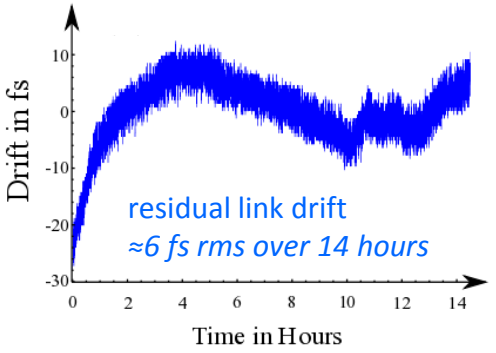

Courtesy of MenloSystems GmbH

Arrival time diagnostics

Bunch Arrival Monitors

- *RF deflectors*
- *Electro-optical BAMs*
- *Electro-optical sampling*

For some special applications RF fields are used ***to deflect*** charged beams more than to accelerate it. Structures called ***RF deflectors*** are designed for this task, mostly based on circular waveguide ***dipole modes TM_{1m} and TE_{1m}*** (mode showing an azimuthal periodicity of order 1) properly iris-loaded (for TW deflectors) or short-circuited (for SW deflecting cavities).

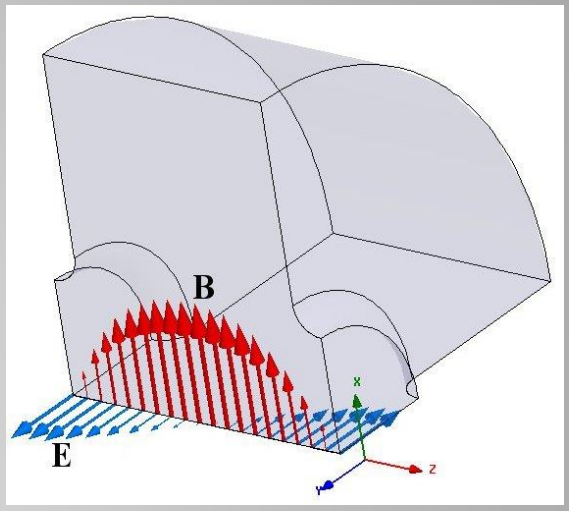

The figure of merit qualifying the efficiency of an RF deflecting structure is the ***transverse shunt impedance*** defined as:

$$R_\perp = \frac{V_\perp^2}{2P} \quad with\ V_\perp = \left| \int_{-L/2}^{L/2} \left[E_y(z) + v B_x(z) \right] e^{j\omega z/c}\, dz \right| = \frac{v}{q} \Delta p_\perp$$

where a deflection in the y-direction for a charge q moving along the z-direction with a velocity v has been considered, and P is the RF power absorbed by the structure.

It turns out that the deflection angle of the charge is:

$$\phi_{def} \approx \frac{\Delta p_\perp}{p} = \frac{qV_\perp}{\beta^2 W}$$

where $p_\perp$ is the transverse component of the momentum $\vec{p}$, and W is the particle energy.

Examples of RF Deflecting Structures

There are many different applications requiring deflecting RF structures:

- Cavities for crab crossing, to obtain head-on bunch collisions in colliders where beam trajectories cross with an angle.
- RF injection kickers, to create closed bump orbits rapidly varying with time in a ring for exotic stacking configuration.
- RF separators, to separate and collect different ion species produced by a source.
- **Diagnostics RF deflectors, for intra-bunch tomography of the longitudinal phase space.**

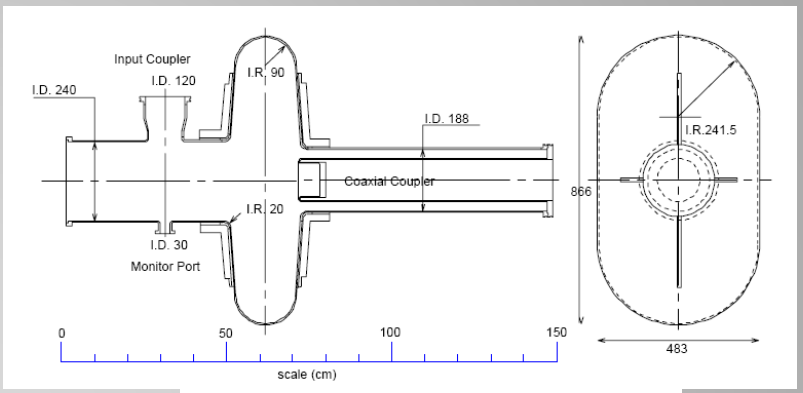

KEK-B SC Crab Cavity

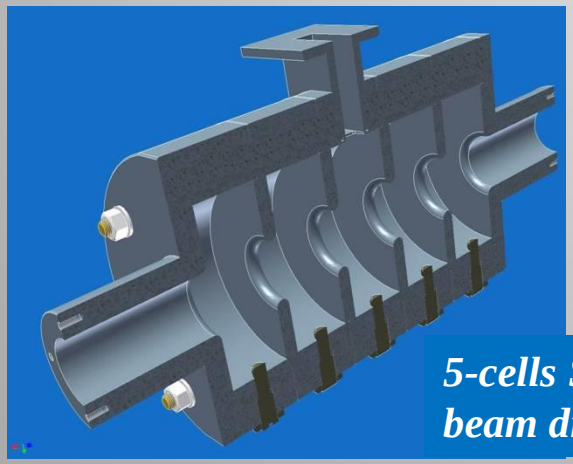

5-cells SW RF Deflector for beam diagnostics at SPARC

TW RF Deflector for CTF3 combiner ring

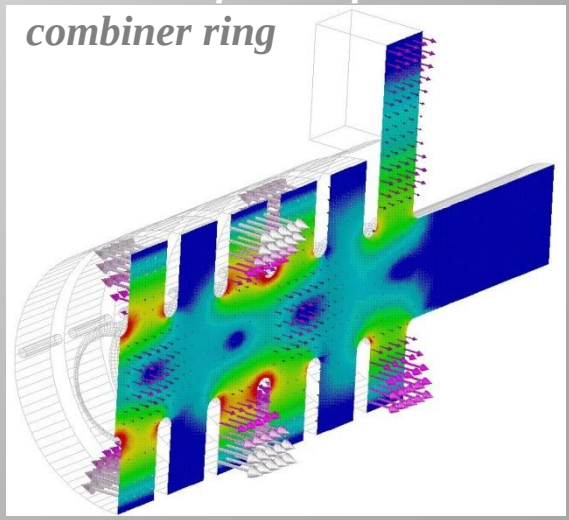

RF deflectors are used for ***beam longitudinal phase space diagnostics*** by simply streaking the bunch on a fluorescent screen applying a ***time dependent transverse kick***. This establishes a correlation between the arrival time t_p of a particle at the deflector and its final transverse position y_s on the screen. For bunch much shorter than the RF wavelength passing near the zero-crossing the correlation is pretty linear. The ***beam image*** on the screen is captured by a camera so that ***longitudinal charge distribution*** and ***centroid longitudinal position*** can be measured.

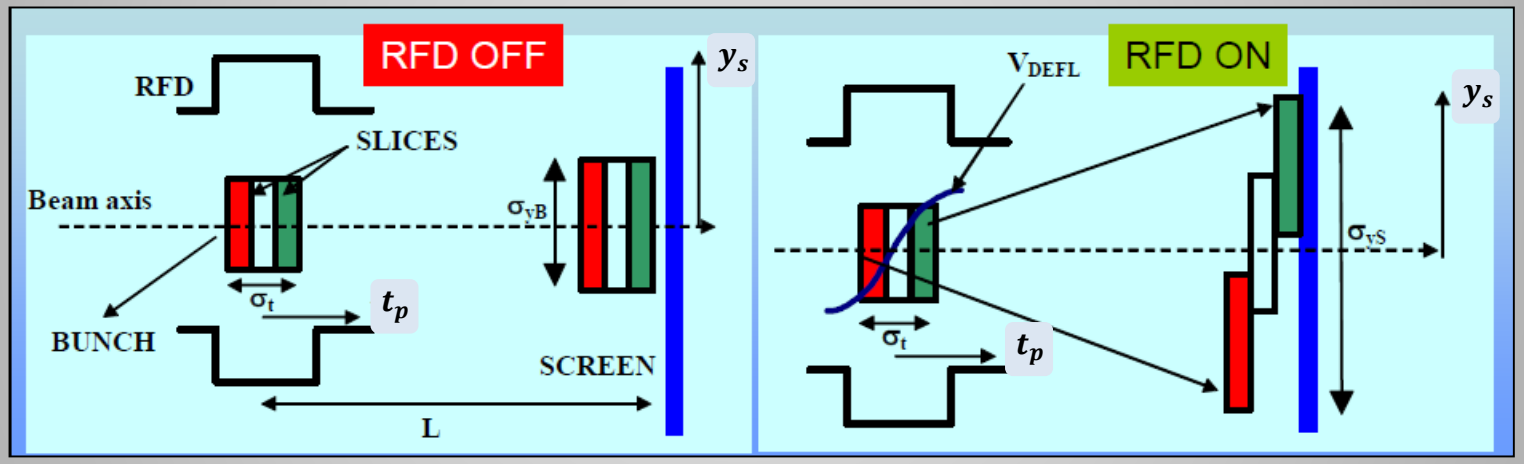

Assuming a free-space beam propagation, elementary cinematics gives the final position on the screen y_s of a relativistic particle entering the deflector at time t with transverse coordinates (y_{def}, y'_{def}):

$$y_s = \frac{V_\perp L}{W/q}\sin[\omega_{RF}(t - t_{RF})] + y'_{def}L + y_{def} \approx \frac{V_\perp \omega_{RF} L}{W/q}(t - t_{RF}) + y'_{def}L + y_{def}$$

$$K_\perp$$

The time-resolution τ_{res} provided by this set up is defined as the minimum arrival time deviation for a particle or a distribution centroid corresponding to a transverse displacement on the screen equal to the natural (RF deflector off) beam spot-size $\sigma_{y_{s0}}$.

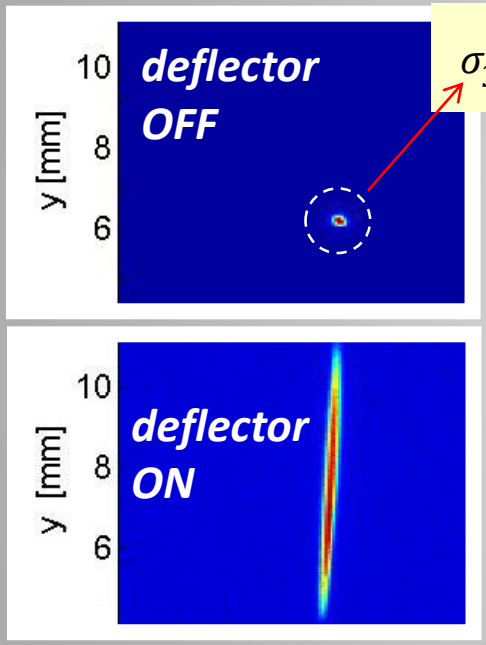

$$\sigma_{y_{s0}}^2 = \langle y_{s0}^2 \rangle = \langle y_{def}^2 \rangle + 2L\langle y_{def}\, y'_{def} \rangle + L^2 \langle (y'_{def})^2 \rangle$$

$\beta_\perp^{defl}\,\varepsilon_\perp$ $\quad -\alpha_\perp^{defl}\,\varepsilon_\perp$ $\quad \gamma_\perp^{defl}\,\varepsilon_\perp$

$\alpha_\perp^{defl}, \beta_\perp^{defl}, \gamma_\perp^{defl}$: *Twiss parameters at the deflector position*

$\varepsilon_\perp$: *beam transv. emittance*

$$\sigma_{y_{s0}}^2 = \frac{\varepsilon_\perp}{\beta_\perp^{defl}} L^2 \left[1 + \left(\frac{\beta_\perp^{defl}}{L} - \alpha_\perp^{defl} \right)^2 \right]$$

$L = \beta_\perp^{defl} / \alpha_\perp^{defl}$ *screen optimal position*

$$\tau_{res} = \frac{\sigma_{y_{s0}}}{K_\perp} = \frac{W/e}{\omega_{RF} V_\perp} \sqrt{\frac{\varepsilon_\perp}{\beta_\perp^{defl}}} \sqrt{1 + \left(\frac{\beta_\perp^{defl}}{L} - \alpha_\perp^{defl} \right)^2} = \frac{W/e}{\omega_{RF} V_\perp} \sqrt{\frac{\varepsilon_\perp}{\beta_\perp^{defl}}}$$

Achievable resolution down to ≈ 10 fs

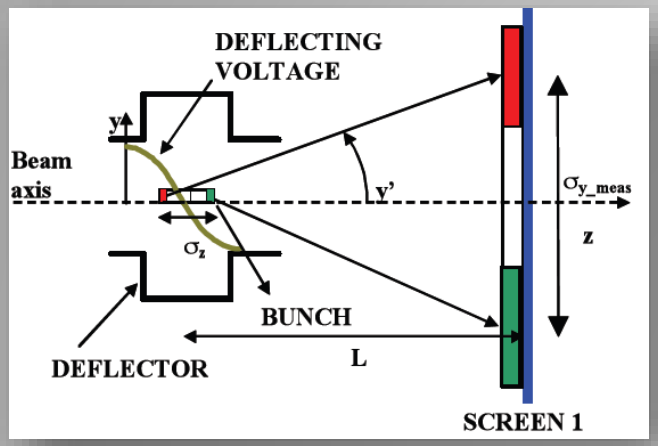

- ✓ Works typically on ***single bunch***. Bunch trains can be eventually resolved with fast gated cameras;
- ✓ ***Destructive*** (needs an intercepting screen ...)
- ✓ Measure bunch ***wrt to deflector RF*** (relative measurement)
- ✓ Longitudinal ***phase space imaging*** with a ***spectrometer*** $(z, \epsilon) \rightarrow (y, x)$
- ✓ ***Off-axis*** particles experience ***accelerating E-field*** (Panofsky-Wenzel theorem) ***proportional*** to ***transverse displacement***. RF deflectors introduce ***energy spread*** correlated with transverse position. The induced relative energy spread increases proportionally to the maximum deflecting angle $qV_\perp/W$ and to the beam transverse dimension at the deflector.

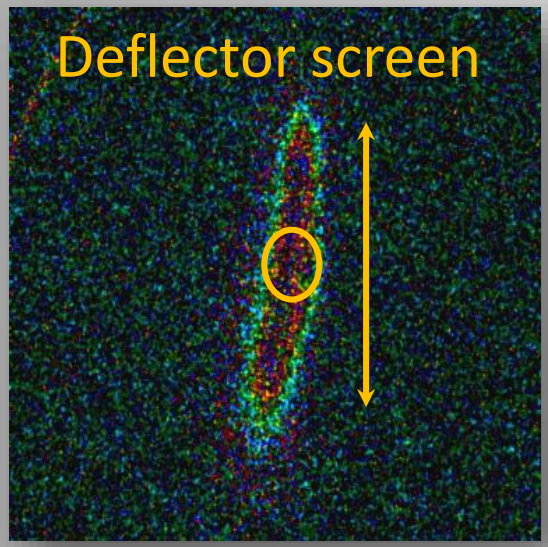

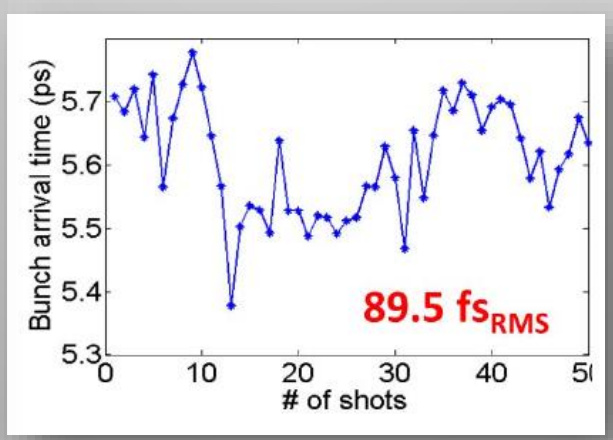

Electro-Optical BAM

The ***electro-optical Bunch Arrival Monitor*** is a device developed at FLASH (DESY) to measure the ***arrival time*** of a ***train of electron bunches*** exploiting the ***large slew rate*** (of the order of 1V/ps) of the voltage delivered by a button ***Beam Position Monitor*** excited by the passage of a short bunch.

The bunch ***arrival time information*** is encoded in the time position of the ***zero-crossing*** of the fastest front of the BPM delivered signal.

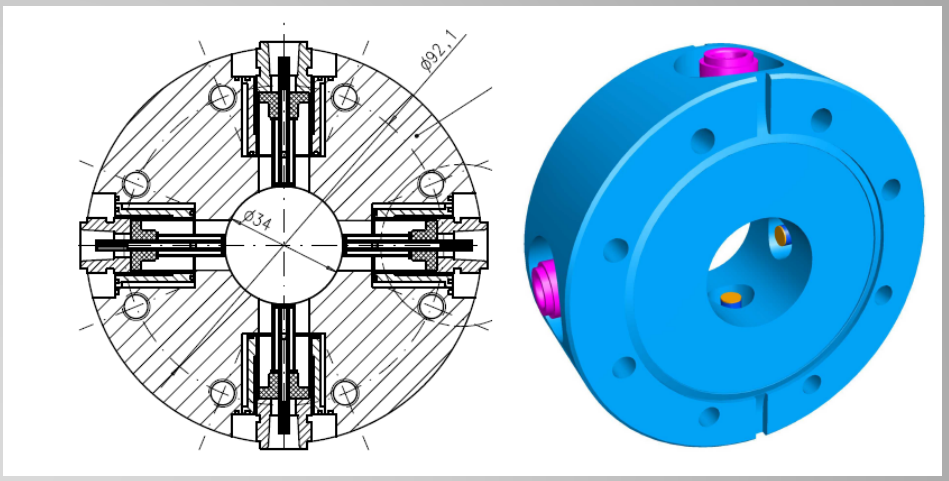

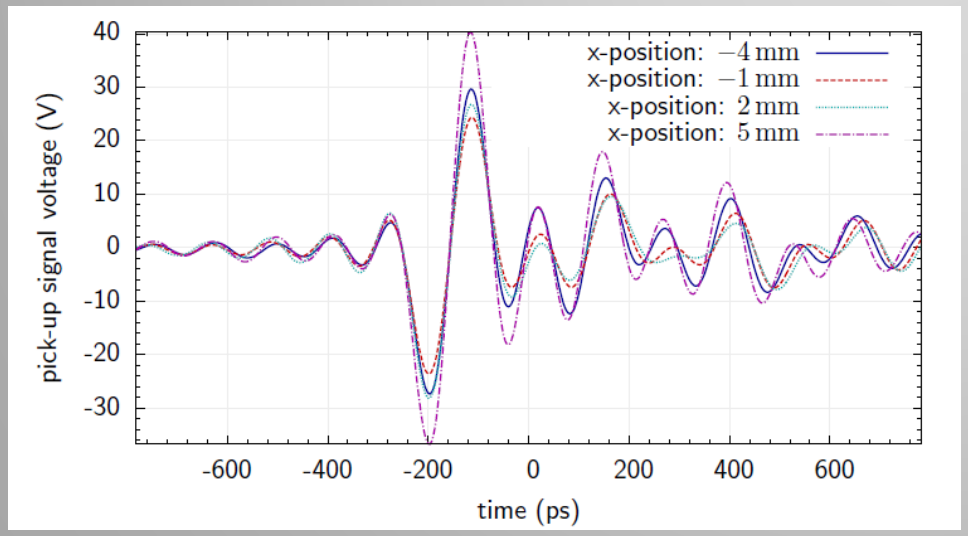

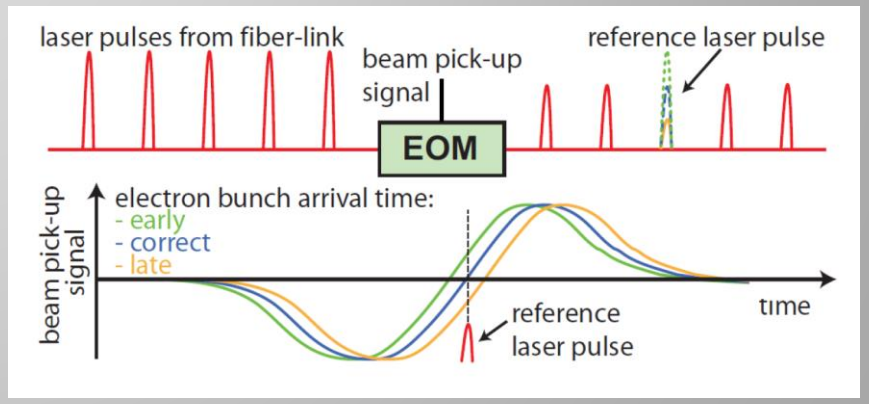

Sketches from ***H. Schlarb*** and ***F. Loehl***

Electro-Optical BAM

A ***reference laser pulse train*** (typically taken from the facility OMO) is connected to the optical input of a ***Mach-Zehnder interferometric modulator*** (***EOM***). The short laser pulses are ***amplitude-modulated*** by the ***button BPM*** signal which is conveniently temporally aligned near to the voltage zero-crossing. ***The bunch arrival time jitter*** and ***drift*** is converted in ***amplitude modulation*** of the laser pulses and measured.

- ✓ *Works very well on bunch trains;*
- ✓ *Non-intercepting;*
- ✓ *Measure bunch wrt to a laser reference (OMO);*
- ✓ *Demonstrated high resolution*

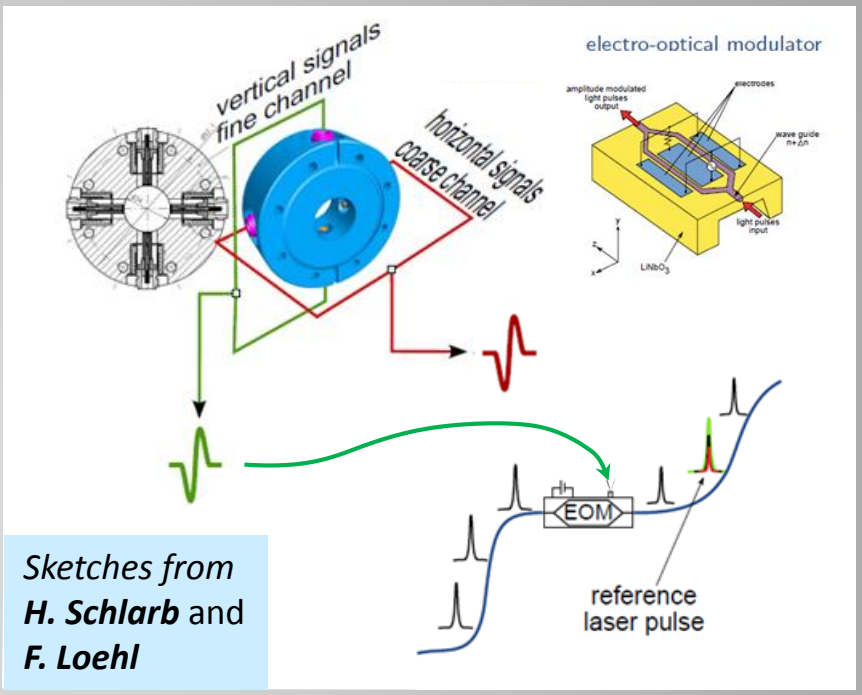

Sketches from ***H. Schlarb*** and ***F. Loehl***

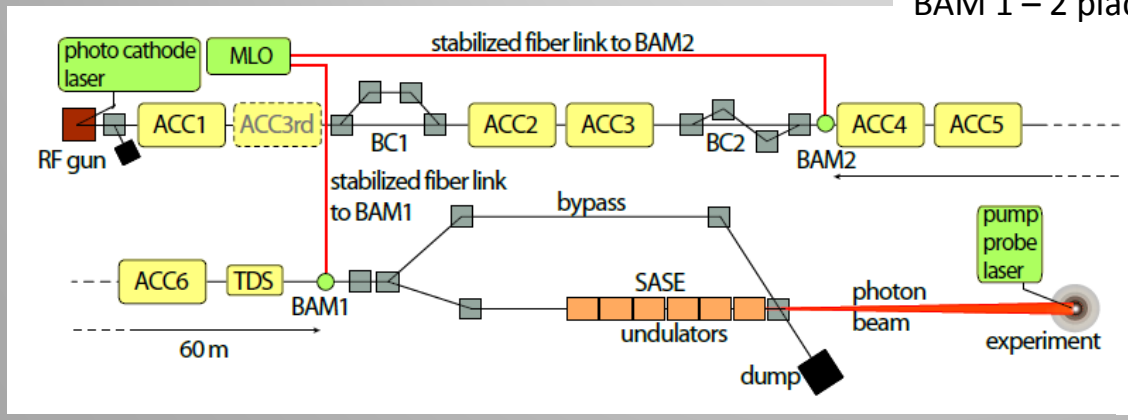

BAM 1 – 2 placed 60 m away along the beam path

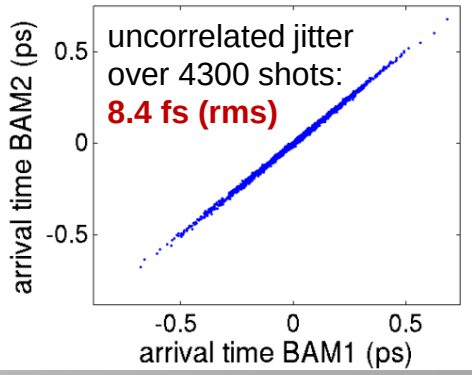

Electro-optical sampling (EOS) is a technique providing information on bunch ***longitudinal charge distribution*** and ***arrival time***.

This technique is based on the property of some ***optically active crystals*** (such as *Zinc Telluride* ***ZnTe,*** *Gallium Phosphide* ***GaP,*** *Gallium Selenide* ***GaSe***) to become ***birefringent*** when exposed to an intense electric field (in the MV/m range when exposed to a particle beam).

The birefringence is an effect proper of anisotropic crystals showing ***different refraction indexes*** for **different orientations** (polarization directions) of the **electric field vector** of an electromagnetic wave propagating through.

As a consequence, a linearly polarized wave (such as a laser pulse) impinging on a birefringent crystal will gain elliptical polarization while propagating along it.

EOS crystal (ZnTe, GaP, GaSe, …)

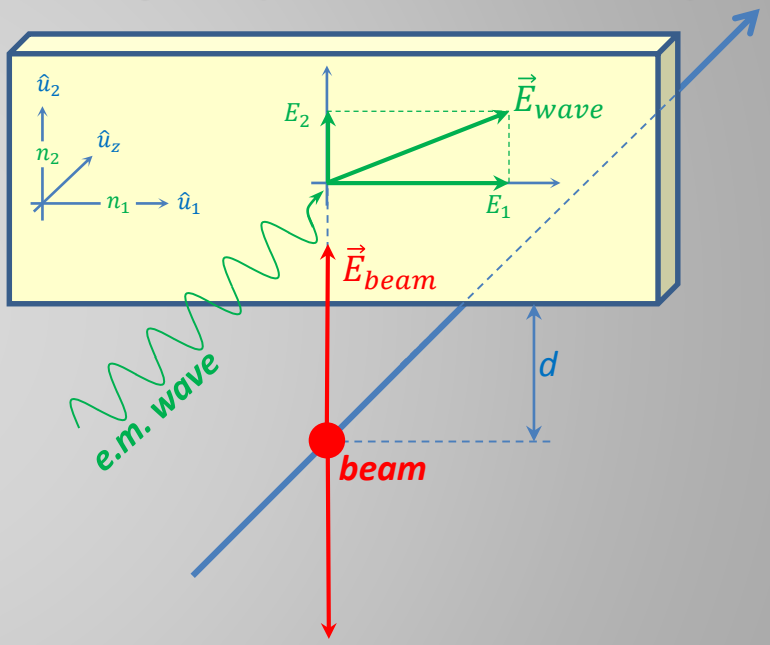

$$\vec{E}_{wave}(z,t) = E_1 \cos[\omega(t - n_1\, z/c)]\, \hat{u}_1 + E_2 \cos[\omega(t - n_2\, z/c)]\, \hat{u}_2$$

An optically active crystal placed in the vicinity of the beam trajectory shows birefringence ***only during the bunch passage*** because of the Lorentz contracted Coulomb electric field travelling with the bunch.

A laser radiation illuminates the crystal, while a ***polarizer P*** and an ***analyzer A*** orthogonally oriented are placed upstream and downstream. In absence of beam, the laser polarization remains unchanged through the crystal (no birefringence) and no radiation can pass through the analyzer A. On the contrary, in presence of a beam the laser intensity downstream the system is modulated by the bunch transverse electric field.

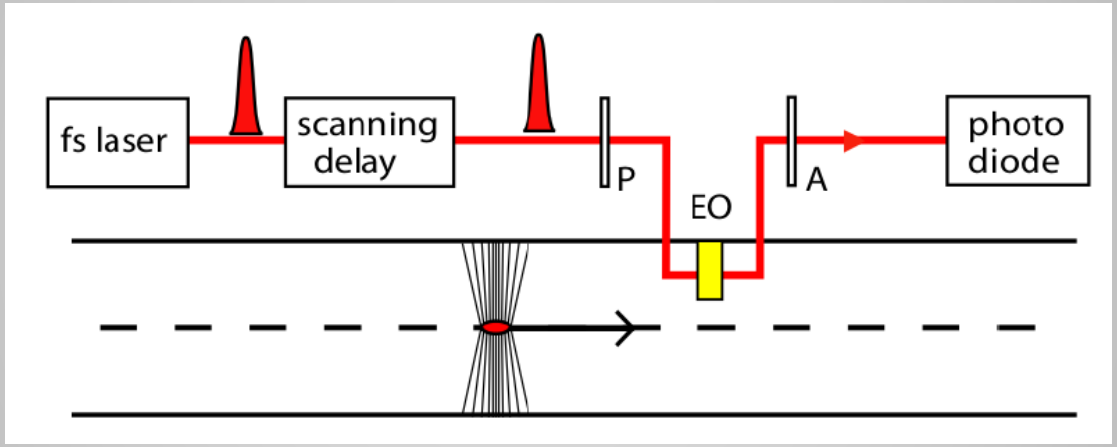

The ***EOS*** is a ***non-intercepting*** technique imprinting an ***intensity modulation*** on a laser pulse ***proportional*** to the bunch current, i.e. to the ***bunch charge longitudinal distribution***. For short bunches (sub picosecond rms duration) the imprinted modulation is too fast (bandwidths extending to the THz region!) to be directly time-resolved in single shot .

A very short laser pulse together with a scanning delay line can be used to sample the bunch distribution in multishot regime. However, ***single shot EOS diagnostics*** is possible by converting the time dependency of the laser intensity into displacement on a screen, and capturing the footprint image by means of a CCD camera.

Translating time into position

Spectrally resolved EOS

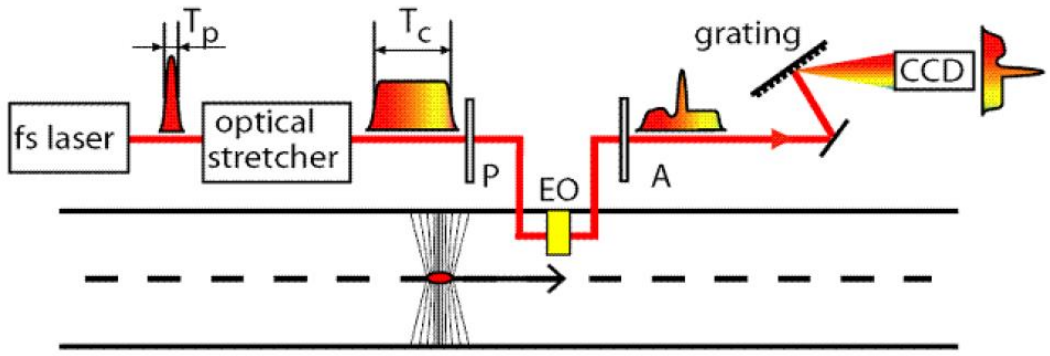

The laser pulse is stretched and linearly chirped before interaction to produce a time-wavelength correlation. The spectral components of the EOS modulated pulse are then resolved by means of a grating.

Limits:

The frequency mixing between the THz and the optical waves broadens the spectral components, limiting the resolution to ≈ 200 fs.

Temporally resolved EOS

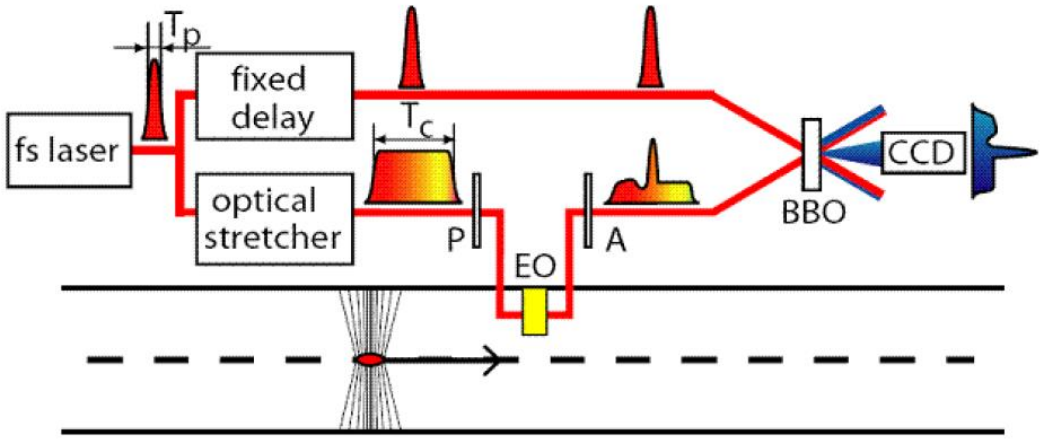

The stretched and intensity modulated EOS pulse is scanned by a copy of the unstretched pulse by performing a large-angle cross-correlation on a non-linear BBO crystal. Because of the crossing angle and the transverse dimensions of the 2 beams, the EOS signal beamlets interact at different transverse positions of the crystal.

Limits:

A quite good resolution of ≈ 50 fs can be achieved but the laser intensity required for x-correlation is substantially higher.

Translating time into position

Spatially resolved EOS

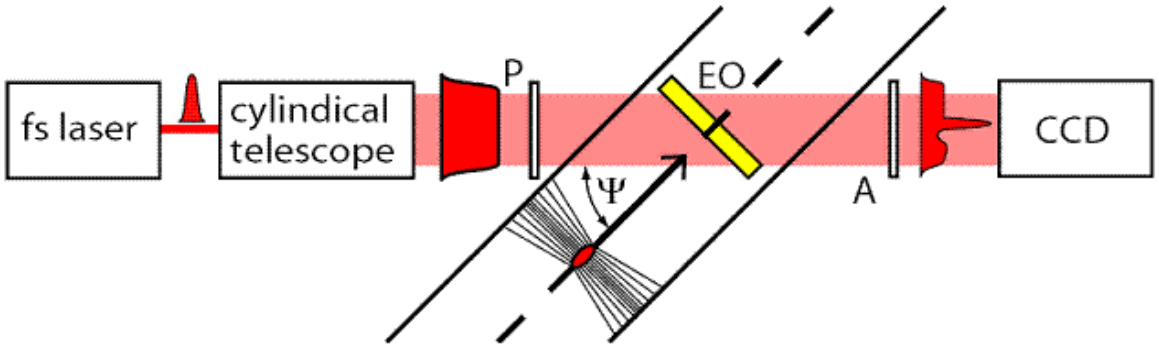

The laser pulse is ***transversally stretched*** and impinges the EOS crystal at a large angle. ***One side*** of the crystal is reached earlier by the laser wavefront and ***samples the bunch head field***, while ***the opposite side*** is reached later and probes the ***bunch tail field***. The image of the laser intensity profile on the screen is directly correlated to the charge longitudinal distribution.

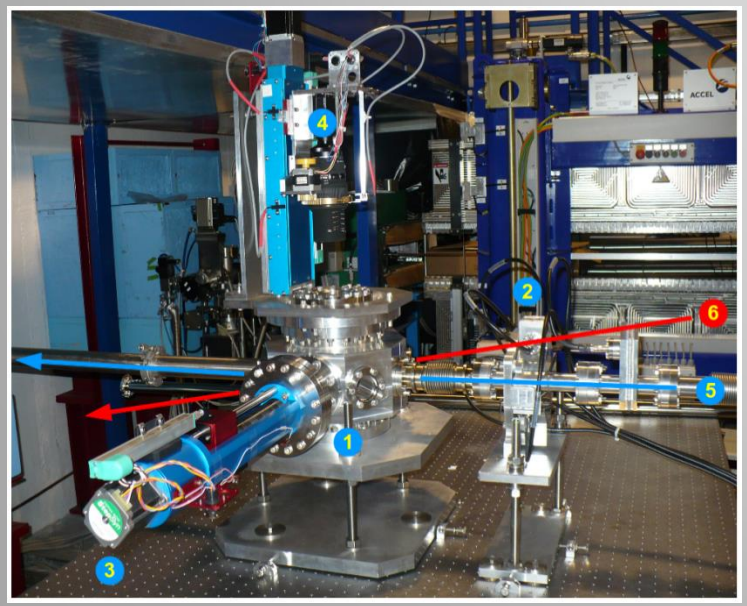

Spatially resolved EOS is the simplest experimental geometry.

The bunch length measurement resolution is ***≈ 50 fs*** and is limited by the material ***dispersion*** that tends to ***enlarge the duration*** of the **beam THz pulse** while travelling across the crystal. This ***only partially affects*** the bunch arrival time measurement (shot-to-shot variation of the distribution centroid).

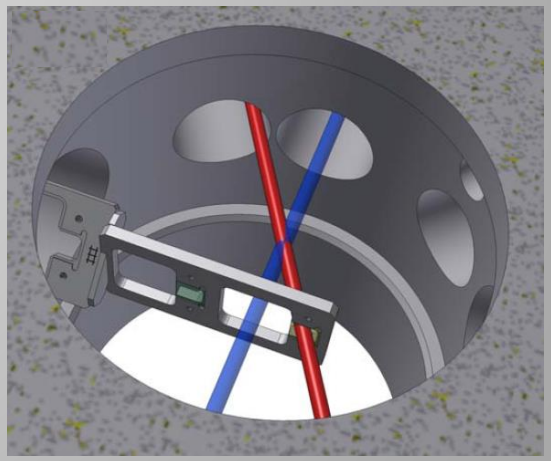

Spatially resolved EOS provides an even better resolution for bunch arrival time diagnostics, at level of: $AT_{res} < 10\ fs$.

EOS beam longitudinal diagnostics summary:

- ✓ Single shot, non-intercepting;
- ✓ Provides charge distribution and centroid position;
- ✓ Resolution $\approx 50\ fs$ for the bunch duration, $< 10\ fs$ for centroid arrival time (*1 pixel ≈ 10 fs*).

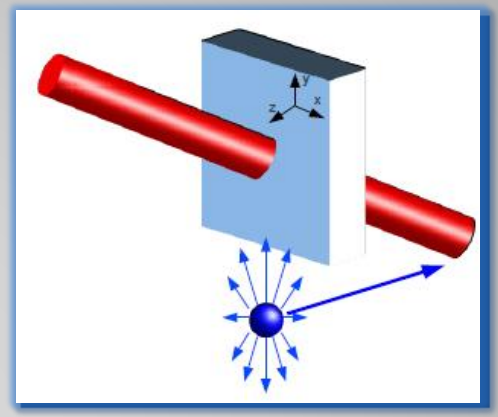

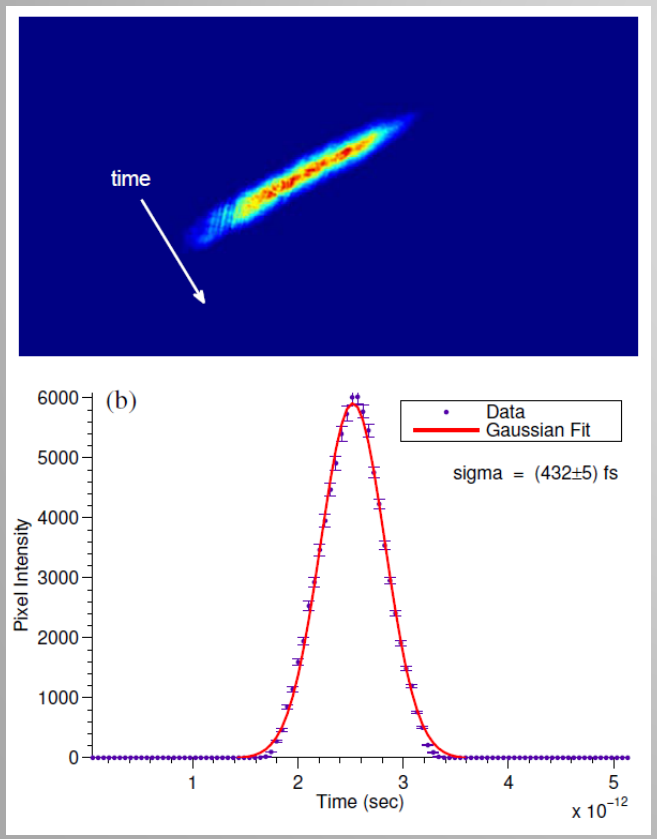

beam ATJ vs. PC laser measured with EOS @SPARC_LAB

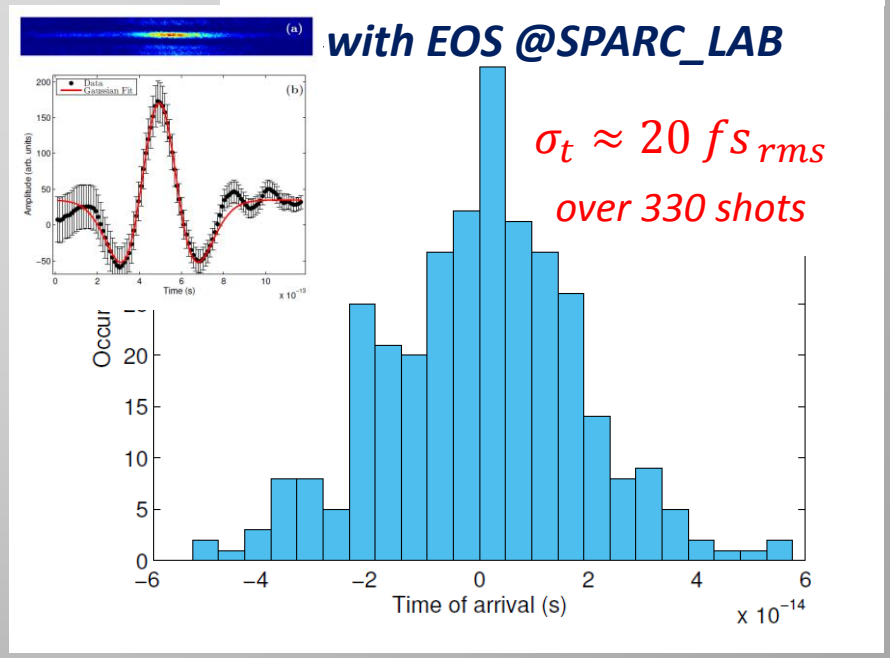

Beam Synchronization

- *Effects of Client Synchronization*
- *Errors on Bunch Arrival Time*

Basics of magnetic bunch compression

sketch from Josef Frisch - SLAC

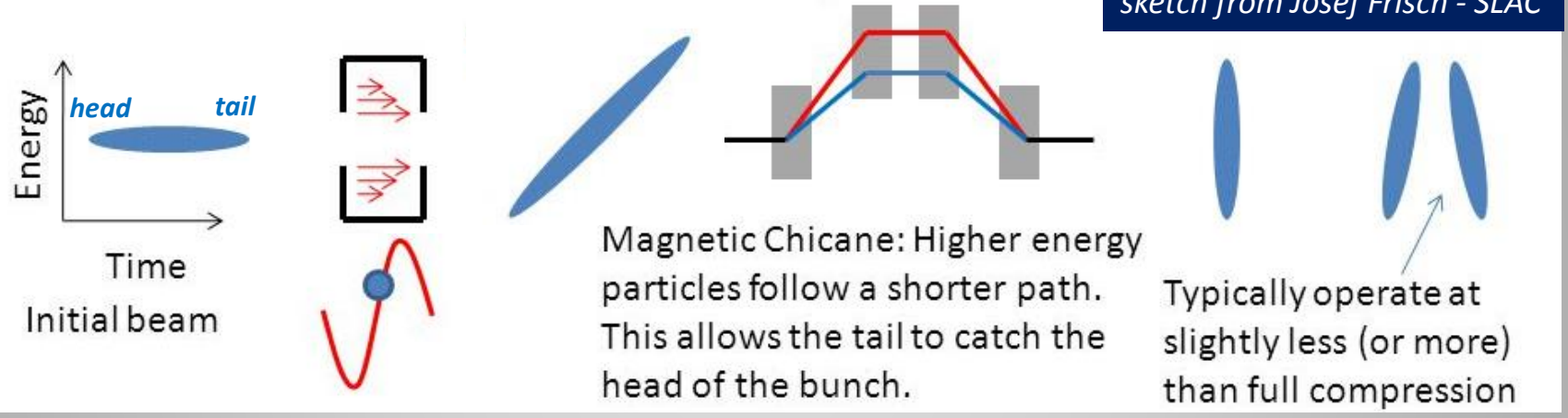

Energy chirp h:

Energy gain through the compressor of a particle starting with proper energy and phase values W_{in} and φ_0

$$W_0 = W_{in} + qV_{RF}\cos(\varphi_0)$$

Final energy error of an accelerated particle starting with energy and phase errors ΔW_{in} and $\Delta\varphi$

$$\Delta W_o = \Delta W_{in} - qV_{RF}\sin(\varphi_0)\,\Delta\varphi = \Delta W_{in} + h\frac{c}{\omega_{RF}}W_0\,\Delta\varphi$$

with

chirp coefficient = relative energy deviation normalized to the particle z position

$$h \overset{\text{def}}{=} \frac{\Delta W/W_0}{\Delta z} = \frac{\omega_{RF}}{c}\frac{\Delta W/W_0}{\Delta\varphi} = \frac{-qV_{RF}\sin(\varphi_0)}{W_{in} + qV_{RF}\cos(\varphi_0)}\frac{\omega_{RF}}{c}$$

Non-isochronous transfer line:

The bunch compression process is completed by making the chirped beam travel along a non-isochronous transfer line. Particles with different energies travel along paths of different lengths according to:

$$\Delta L = R_{56}(\Delta W_0/W_0)$$

Path elongation normalized to the relative energy error

Overall, a particle entering the magnetic compressor with a time error Δt_{in} and a relative energy error $\Delta W_{in}/W_{in}$ will leave it with time and relative energy errors $\Delta W_o/W_o$ and Δt_o given by:

$$\Delta W_0/W_0 = hc\,\Delta t_{in} + \frac{W_{in}}{W_0}\Delta W_{in}/W_{in}$$

$$\Delta t_o = \Delta t_{in} + \frac{\Delta L}{c} = \Delta t_{in} + \frac{R_{56}}{c}(\Delta W_0/W_0) = (1 + h\,R_{56})\Delta t_{in} + \frac{R_{56}}{c}\frac{W_{in}}{W_0}(\Delta W_{in}/W_{in})$$

In the end if the compressor is tuned to get $h \cdot R_{56} \approx -1$ it may easily noticed that the exit time of a particle is almost independent on the entering time. This mechanism describes the deformation (compression) of the longitudinal distribution of the particles in a bunch, ***but also the multi-shot dynamics of the bunch center of mass***. ***The bunch arrival time downstream the compressor is weakly related to the upstream arrival time***.

Compressor longitudinal transfer matrices:

Previous results can be summarized in a matrix notation, according to:

$$\begin{pmatrix} \Delta t \\ \Delta W/W \end{pmatrix}_o = \begin{bmatrix} 1 & \frac{R_{56}}{c} \\ 0 & 1 \end{bmatrix} \begin{bmatrix} 1 & 0 \\ hc & \frac{W_{in}}{W_0} \end{bmatrix} \begin{pmatrix} \Delta t \\ \Delta W/W \end{pmatrix}_{in} = \begin{bmatrix} 1+hR_{56} & \frac{R_{56}}{c}\frac{W_{in}}{W_0} \\ hc & \frac{W_{in}}{W_0} \end{bmatrix} \begin{pmatrix} \Delta t \\ \Delta W/W \end{pmatrix}_{in}$$

$\hat{B}$ non-isochronous drift

$\hat{A}$ chirping acceleration

$\hat{C} = \hat{B} \cdot \hat{A}$ total compressor stage

Effects of PM and AM in the compressor RF on final bunch energy and arrival time:

Let's consider now the presence of phase ($\Delta\varphi_o = -\omega_{RF}\Delta t_{RF}$) and amplitude ($\Delta V_{RF}/V_{RF}$) errors in the RF section of the compressor. The resulting energy error of the beam entering in the non-isochronous drift is:

$$\Delta W_o = q\Delta V_{RF}\cos(\varphi_o) - qV_{RF}\sin(\varphi_o)\Delta\varphi_o$$

$$\frac{\Delta W_o}{W_o} = -hc\Delta t_{RF} + \frac{W_o - W_{in}}{W_o}\frac{\Delta V_{RF}}{V_{RF}}$$

The energy error will result in a time error downstream the drift through the transfer matrix $\hat{B}$.

$$\begin{pmatrix} \Delta t \\ \Delta W/W \end{pmatrix}_o = \begin{bmatrix} 1 & \frac{R_{56}}{c} \\ 0 & 1 \end{bmatrix} \begin{bmatrix} 0 & 0 \\ -hc & \frac{W_0 - W_{in}}{W_0} \end{bmatrix} \begin{pmatrix} \Delta t_{RF} \\ \Delta V_{RF}/V_{RF} \end{pmatrix} = \begin{bmatrix} -hR_{56} & \frac{R_{56}}{c}\frac{W_0 - W_{in}}{W_0} \\ -hc & \frac{W_0 - W_{in}}{W_0} \end{bmatrix} \begin{pmatrix} \Delta t_{RF} \\ \Delta V_{RF}/V_{RF} \end{pmatrix}$$

$\hat{B}$ non-isochronous drift

$\hat{N}$ RF noise-to-energy

$\hat{R} = \hat{B} \cdot \hat{N}$ RF AM&PM conversion to bunch time and energy

BC block diagram:

To the first order the RF noise does not affect the bunch internal distribution, since RF amplitude and phase does not change significantly over a bunch time duration. It will more affect the bunch-to-bunch energy deviation and arrival time.

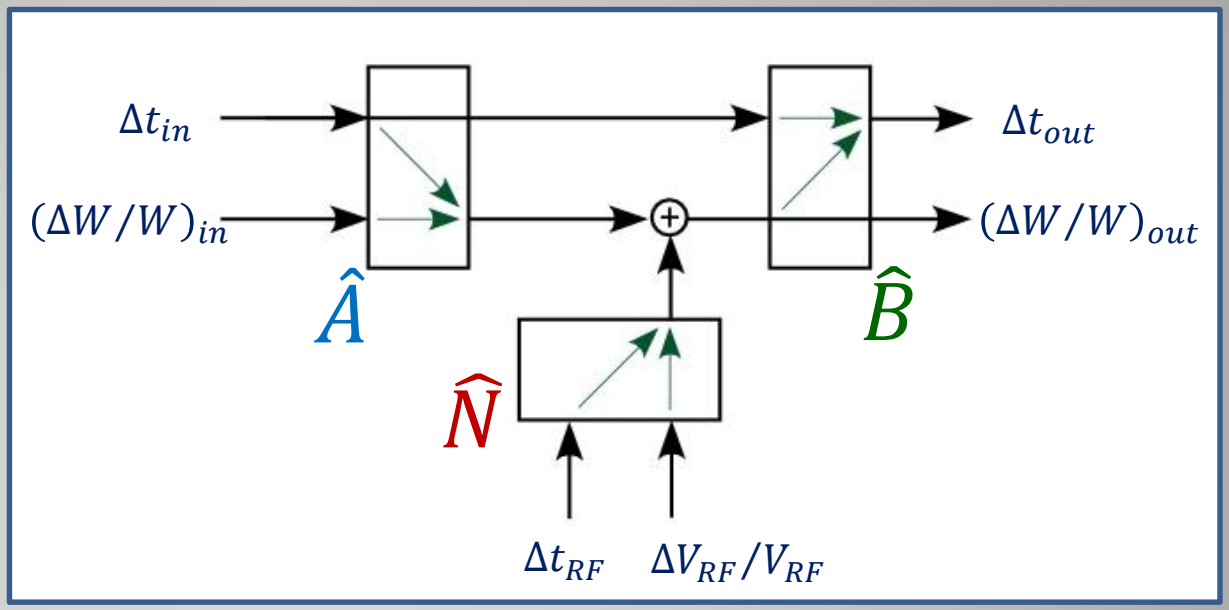

$$\begin{pmatrix} \Delta t \\ \Delta W/W \end{pmatrix}_0 = \hat{B}\left[\hat{A}\begin{pmatrix} \Delta t \\ \Delta W/W \end{pmatrix}_{in} + \hat{N}\begin{pmatrix} \Delta t_{RF} \\ \Delta V_{RF}/V_{RF} \end{pmatrix}\right]$$

$$\Delta t_0 = \underbrace{(1 + hR_{56})}_{\approx 0}\Delta t_{in} \underbrace{- hR_{56}}_{\approx 1}\Delta t_{RF} + \frac{R_{56}}{c}\frac{W_{in}}{W_0}(\Delta W/W)_{in} + \frac{R_{56}}{c}\frac{W_0 - W_{in}}{W_0}(\Delta V_{RF}/V_{RF})$$

The bunch arrival time downstream the compressor is strongly related to the phase of the chirping RF. It is also affected by initial energy errors and RF amplitude variations.

Beam synchronization

How beam arrival time is affected by synchronization errors of the sub-systems?

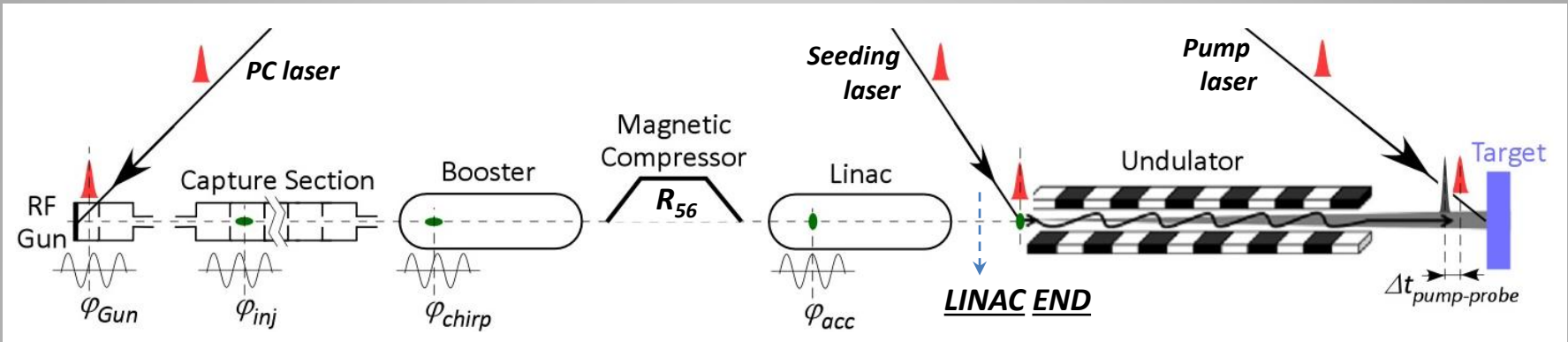

Perfect synchronization: the time (or phase) T_i of all sub-systems properly set to provide required beam characteristics at the Linac end, where the bunch centroid arrives at time T_b.

Perturbations of subsystem phasing Δt_i will produce a change Δt_b of the beam arrival time.

First-order approximation:

$$\Delta t_b = \sum_i a_i \, \Delta t_i = \sum_i \frac{\Delta t_i}{c_i} \qquad with \qquad \sum_i a_i = 1$$

Compression coefficients

The introduced a_i coefficients express the ***weights*** of the various clients in ***determining*** the ***beam arrival time***. Values of a_i can be computed analytically, by simulations or even measured experimentally. They very much depends on the machine working point.

Beam synchronization

How beam arrival time is affected by synchronization errors of the sub-systems?

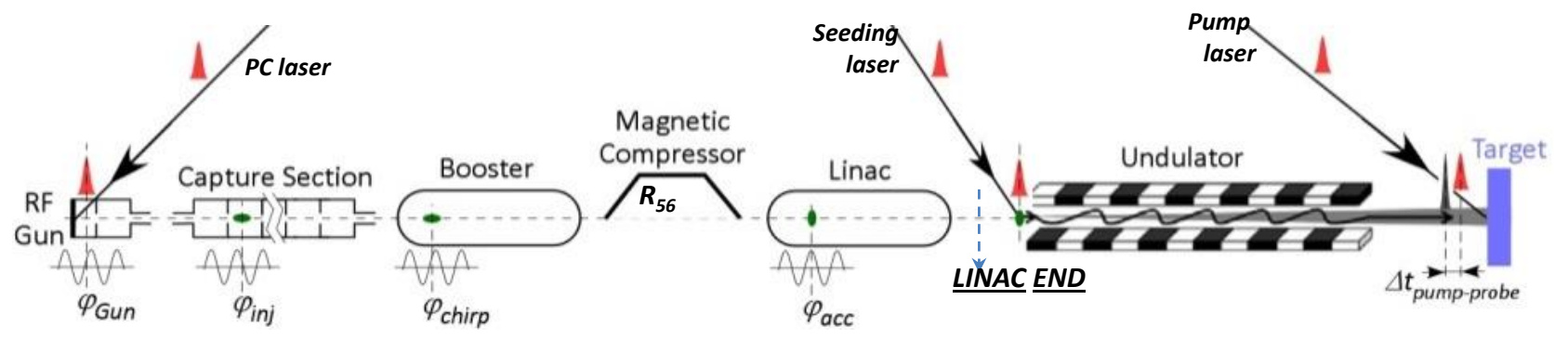

Dependence of the weighting coefficients a_i on the machine working point

1. No compression: Beam captured by the GUN and accelerated on-crest

$$a_{PC} \approx 0.6 \div 0.7\,; \qquad a_{RF_{GUN}} \approx 0.4 \div 0.3\,; \qquad others\ a_i \approx 0$$

2. Magnetic compression: Energy-time chirp imprinted by off-crest acceleration in the booster and exploited in magnetic chicane to compress the bunch

$$a_{RF_{boost}} \approx 1\,; \qquad |a_{PC}| \ll 1\,; \qquad others\ a_i \approx 0$$

Compression can be staged (few compressors acting at different energies). Bunch can be overcompressed, i.e. head and tail are reversed ($a_{RF_{boost}} > 1, a_{PC} < 0$).

Beam synchronization

How beam arrival time is affected by synchronization errors of the sub-systems?

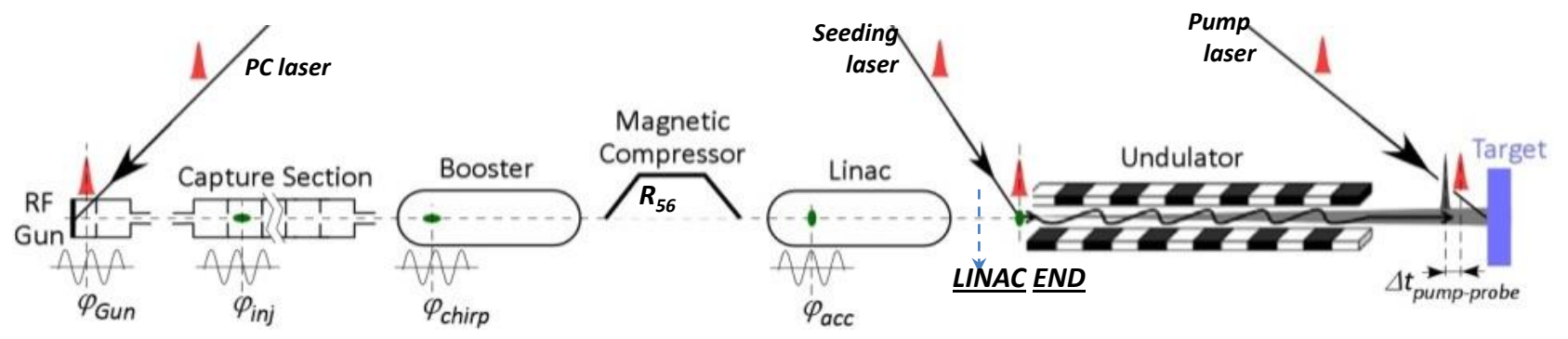

Dependence of the weighting coefficients a_i on the machine working point

3. RF compression: a non fully relativistic bunch ($E_0 \approx few\ MEV$ at Gun exit) injected ahead the crest in an RF capture section slips back toward an equilibrium phase closer to the crest during acceleration, being also compressed in this process

$$a_{RF_{CS}} \approx 1\ ; \qquad |a_{PC}|, |a_{RF_{GUN}}| \ll 1; \qquad others\ a_i \approx 0$$

The bunch gains also an Energy-time chirp. RF and magnetic compressions can be combined.

Particle distribution within the bunch and shot-to-shot centroid distribution behave similarly, but values of coefficients a_i might be different since space charge affects the intra-bunch longitudinal dynamics.

Beam synchronization

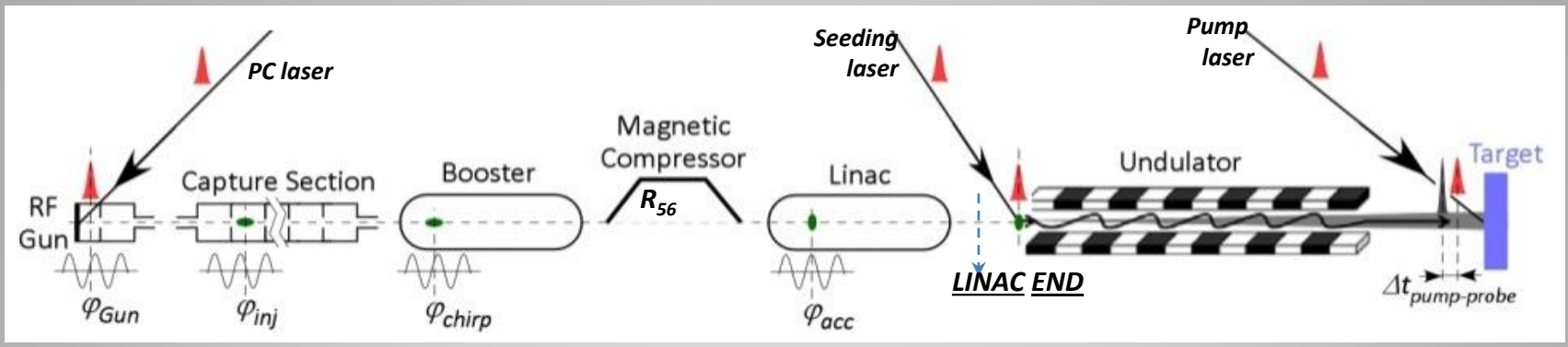

Bunch Arrival Time Jitter

If we consider uncorrelated residual jitters of Δt_i (measured wrt the facility reference clock), the bunch arrival time jitter σ_{t_b} is given by:

$$\sigma_{t_b}^2 = \sum_i a_i^2 \, \sigma_{t_i}^2$$

while the jitter of the beam respect to a specific facility sub-system (such as the PC laser or the RF accelerating voltage of a certain group of cavities) $\sigma_{t_{b-j}}$ is:

$$\Delta t_{b-j} = \Delta t_b - \Delta t_j = (a_j - 1)\Delta t_j + \sum_{i \neq j} a_i \, \Delta t_i$$

$$\sigma_{t_{b-j}}^2 = (a_j - 1)^2 \sigma_{t_j}^2 + \sum_{i \neq j} a_i^2 \, \sigma_{t_i}^2$$

Beam synchronization

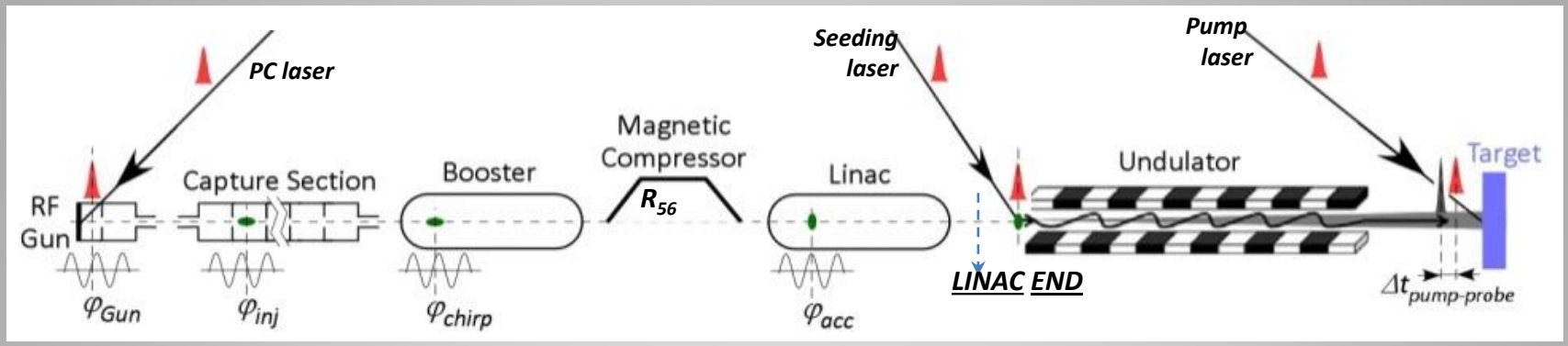

Bunch Arrival Time Jitter

NUMERICAL EXAMPLE: PC laser jitter $\sigma_{t_{PC}} \approx 70\ fs$, RF jitter $\sigma_{t_{RF}} \approx 30\ fs$

No Compression: $a_{PC} \approx 0.65,\ a_{RF_{GUN}} \approx 0.35$

$$\sigma_{t_b} \approx 47\ fs$$
$$\sigma_{t_{b-PC}} \approx 27\ fs;\ \sigma_{t_{b-RF}} \approx 50 fs$$

Magnetic Compression: $a_{PC} \approx 0.2,\ a_{RF_{boost}} \approx 0.8$

$$\sigma_{t_b} \approx 28\ fs$$
$$\sigma_{t_{b-PC}} \approx 61\ fs;\ \sigma_{t_{b-RF}} \approx 15 fs$$

CONCLUSIONS

- ✓ Timing and Synchronization has growth considerably in the last ~ 15 years as a Particle Accelerators specific discipline
- ✓ It involves concepts and competences from various fields such as Electronics, RF, Laser, Optics, Control, Diagnostics, Beam dynamics, …
- ✓ Understanding the real synchronization needs of a facility and proper specifications of the systems involved are crucial for successful design and efficient operation (but also to avoid overspecification leading to extra-costs and unnecessary complexity ...)
- ✓ Synchronization diagnostics (precise arrival time monitors) is fundamental to understand beam behavior and to provide input data for beam-based feedback systems correcting synchronization residual errors
- ✓ Although stability down to the *fs* scale has been reached, many challenges still remain since requirements get tighter following the evolution of the accelerator technology. There are ideas to go further to the attosecond frontier … (*see A. Ferran Pousa et al 2017 J. Phys.: Conf. Ser. 874 012032*)

REFERENCES #1

- F. Loehl, *Timing and Synchronization*, Accelerator Physics (Intermediate level) – Chios, Greece, 18 - 30 September 2011 – slides on web
- H. Schlarb , *Timing and Synchronization*, Advanced Accelerator Physics Course – Trondheim, Norway, 18– 29 August 2013 - slides on web
- M. Bellaveglia, *Femtosecond synchronization system for advanced accelerator applications*, IL NUOVO CIMENTO, Vol. 37 C, N. 4, 10.1393/ncc/i2014-11815-2
- E. Rubiola, *Phase Noise and Frequency Stability in Oscillators,* Cambridge University Press
- E. Rubiola, R. Boudot, *Phase Noise in RF and Microwave Amplifiers,* slides @ http://www.ieee-uffc.org/frequency-control/learning/pdf/Rubiola-Phase_Noise_in_RF_and_uwave_amplifiers.pdf
- O. Svelto, *Principles of Lasers,* Springer
- R.E. Collin, *Foundation for microwave engineering*, Mc Graw-Hill int. editions
- H.Taub, D.L. Schilling, *Principles of communication electronics*, Mc Graw-Hill int. student edition
- J. Kim et al. , *Long-term stable microwave signal extraction from mode-locked lasers*, 9 July 2007 / Vol. 15, No. 14 / OPTICS EXPRESS 8951
- T. M. Hüning et al. , *Observation of femtosecond bunch length using a transverse deflecting structure*, Proc of the 27th International Free Electron Laser Conference (FEL 2005), page 538, 2005.
- R. Schibli et al. , *Attosecond active synchronization of passively mode-locked lasers by balanced cross correlation*, Opt. Lett. 28, 947-949 (2003)
- F. Loehl et al., *Electron Bunch Timing with Femtosecond Precision in a Superconducting Free-Electron Laser,* Phys. Rev. Lett. 104, 144801
- I. Wilke et al. , *Single-shot electron-beam bunch length measurements*, Physical review letters, 88(12) 124801, 2002

REFERENCES #2

- S. Schulz et al., *An optical cross -correlator scheme to synchronize distributed laser systems at FLASH* , THPC160, Proceedings of EPAC08, Genoa, Italy
- F. Loehl, *Optical Synchronization of a Free-Electron Laser with Femtosecond Precision*, PhD Dissertation, http://inspirehep.net/record/833726/files/desy-thesis-09-031.pdf
- M. K. Bock, *Recent developments of the bunch arrival time monitor with femtosecond resolution at FLASH*, WEOCMH02, Proceedings of IPAC'10, Kyoto, Japan
- http://www.onefive.com/ds/Datasheet%20Origami%20LP.pdf
- E5052A signal source analyzer, http://www.keysight.com/en/pd-409739-pn-E5052A/signal-source-analyzer-10-mhz-to-7-265-or-110-ghz?cc=IT&lc=ita
- Menlo Systems GMBH: http://www.menlosystems.com/products/?families=79
- Andrew cables: http://www.commscope.com/catalog/wireless/product_details.aspx?id=1344
- http://www.nist.gov/
- http://www.thinksrs.com/index.htm
- http://www.mrf.fi/
- http://www.sciencedirect.com/science/article/pii/S0168583X13003844
- http://spie.org/Publications/Proceedings/Paper/10.1117/12.2185103
- A Ferran Pousa et al 2017 J. Phys.: Conf. Ser. 874 012032